THESIS FOR THE DEGREE OF DOCTOR OF PHILOSOPHY

Amyloid β and Extracellular Vesicles in Alzheimer's Disease

VESA HALIPI

Department of Life Sciences

CHALMERS UNIVERSITY OF TECHNOLOGY

Gothenburg, Sweden 2026

Amyloid β and Extracellular Vesicles in Alzheimer's Disease

VESA HALIPI
ISBN 978-91-8103-370-0

Doktorsavhandlingar vid Chalmers tekniska högskola
Ny serie nr 5827
ISSN 0346-718X

Department of Life Sciences
Chalmers University of Technology
SE-412 96 Gothenburg
Sweden
Telephone + 46 (0)31-772 1000

Cover:
The illustration depicts EV formation and release into the extracellular space either through fusion of multivesicular bodies with the plasma membrane (exosomes) or via outward budding of the plasma membrane (ectosomes). These EVs interact with and inhibit Aβ aggregation. In turn, Aβ can be taken up by cells in both soluble and fibrillar forms and trafficked through the endolysosomal system, thereby influencing EV release and properties.

Chalmers digitaltryck
Gothenburg, Sweden 2026

Amyloid β and Extracellular Vesicles in Alzheimer's Disease

VESA HALIPI
Department of Life Sciences
Chalmers University of Technology

ABSTRACT

Alzheimer's disease (AD) is a devastating neurodegenerative disorder that is characterized by progressive neuronal loss and associated cognitive decline. Protein aggregation and extracellular deposition of amyloid-β (Aβ) fibrils is a central pathological hallmark of AD, but, prior to Aβ plaque deposition, Aβ can also accumulate intracellularly. This has been linked to endolysosomal dysfunction. Although Aβ as a driver of AD pathology is well established, the exact events that initiate Aβ pathology and drive disease progression remain unclear. This makes the development of effective disease-modifying treatments a major unresolved challenge. Better understanding of the cellular and molecular mechanisms that underlie Aβ pathology is therefore needed.

This thesis aims to clarify the role of extracellular vesicles (EVs) in Aβ aggregation and accumulation, focusing on the disease-associated Aβ(1-42) variant. EVs are cell-secreted vesicles that have been implicated in cell-cell propagation of Aβ and as potential modulators of Aβ plaque formation and toxicity. My work shows that EVs, independent of their cell-origin, delay *in vitro* Aβ(1-42) aggregation by interfering with the fibril elongation step. This drives the formation of short fibrils that could be neurotoxic. To better understand EV-mediated aggregation inhibition, I examined how surface-associated proteins, carbohydrates and lipids contribute. I found that removal of EV surface proteins and, albeit to a considerably lesser extent, carbohydrates, enhances the aggregation inhibitory effect. This suggests that the EV limiting membrane is a significant modulator of Aβ(1–42) aggregation but that its effect can be masked or counteracted by other EV surface biomolecules. This notion was supported by a study on synthetic lipid vesicles which, furthermore, pointed out the importance of lipid raft-like microdomains and ganglioside clustering. Finally, I report on a bidirectional crosstalk between endolysosomal Aβ(1–42) and EVs whereby Aβ(1–42) accumulation alters the EV proteome and enhances EV release in a way that potentiates the aggregation effect and, in turn, further enhances Aβ(1–42) intraneuronal accumulation.

Altogether, this thesis contributes new insights into how EVs modulate Aβ(1–42) self-assembly and accumulation in Alzheimer's disease. This work is important for understanding the basic mechanisms that drive Aβ pathology, and, ultimately, for development of effective therapeutics.

Keywords: Alzheimer's disease, amyloid-β, Aβ(1-42), protein aggregation, amyloid fibrils, extracellular vesicles, lipid vesicle, kinetics

List of publications

This thesis is based on the work contained in the following research papers:

I. Extracellular vesicles slow down Aβ(1-42) aggregation by interfering with the amyloid fibril elongation step
Vesa Halipi, Nima Sasanian, Julia Feng, Jing Hu, Quentin Lubart, David Bernson, Daniel van Leeuwen, Doryaneh Ahmadpour, Emma Sparr and Elin K. Esbjörner
ACS Chemical Neuroscience, (2024).6;15(5):944-954 doi:10.1021/acschemneuro.3c00655

II. Surface proteins modulate extracellular vesicle mediated inhibition of Aβ(1-42) aggregation
Vesa Halipi, Georgia Daoutsali, André Görgens, Samir El Andaloussi, Elin K. Esbjörner
Manuscript

III. Ganglioside GM1 slows down Aβ(1-42) aggregation by a primary nucleation inhibitory mechanism that is modulated by sphingomyelin and cholesterol
Nima Sasanian, Vesa Halipi, Mikaela Sjögren, Johannes Bengtsson, David Bernson, Elin K. Esbjörner
Communications Chemistry, (2025). 13;9(1):39. doi: 10.1038/s42004-025-01846-y

IV. Crosstalk between Aβ(1-42) and extracellular vesicles modulate cell uptake, fibril formation, and vesicle release
Vesa Halipi, Viktoria de Carvalho, Ermir Zulfaj, Quentin Lubart, David Bernson, Elin K. Esbjörner
Manuscript

Contribution report

My contribution to the papers in this thesis is as follows:

I. I conceived the idea and designed the study together with E.K.E. I performed all experiments except the cryo-TEM imaging. I analysed the data together with E.K.E and with input from N.S. I wrote the paper together with E.K.E.

II. I conceived the idea together with E.K.E and designed the study. I performed experiments together with, and supervised, G.D. I analysed and interpreted the data and wrote the paper together with E.K.E.

III. I analysed and fitted the kinetic data and performed some of the aggregation kinetics experiments. I contributed to the analysis and interpretation of the results and I participated in writing the paper together with N.S and E.K.E.

IV. I conceived the idea together with E.K.E and designed the study. I performed all experiments, except the nanochannel analysis and part of the confocal imaging. I analysed and interpreted the data and wrote the paper together with E.K.E.

PREFACE

This dissertation is submitted for the partial fulfilment of the degree of Doctor of Philosophy. The original work presented in this thesis was carried out between September 2021 and February 2026 at Chalmers University of Technology, Department of Life Sciences, under the supervision of Associate Professor Elin K. Esbjörner. The research was funded by the Knut and Alice Wallenberg foundation Academy Fellow (2019.0238).

Vesa Halipi

February 2026

Table of Contents

1. Introduction 1
2. Proteins and Amyloid Fibrils 3
2.1. Protein Folding and Misfolding 3
2.2 Amyloid Fibrils 4
2.3 Amyloid Aggregation 5
3. Alzheimer's Disease 8
3.1 The Aβ Peptide 8
3.2 Aβ Aggregation 10
3.3 Aβ Pathology 11
4 Extracellular Vesicles 12
4.1 EV Biogenesis and Composition 12
4.2 Cellular Uptake of Extracellular Vesicles 14
4.3 Extracellular Vesicles and Aβ Pathology 14
4.3.1 Lipids and Aβ 15
5. Methodology 17
5.1 Aβ Recombinant Protein Expression and Purification 17
5.2 Aβ Aggregation Kinetics 17
5.2.1 Mechanistic models and analysis of Aβ aggregation kinetics 18
5.3 Microscopy 20
5.3.1 Atomic force microscopy 20
5.3.2 Confocal microscopy 21
5.4 Flow Cytometry 22
5.5 EV Isolation and Characterization 23
5.5.1 Ultrafiltration and tangential flow filtration 24
5.5.2 Nanoparticle tracking analysis 24
6. Original Work 25
6.1 Extracellular vesicles slow down Aβ fibril formation and alter Aβ fibril morphology 25
6.2 The role of proteins, proteoglycans and lipids in EV - Aβ interactions 30
6.2.1 Surface proteins modulate the EV-mediated inhibition of Aβ(1-42) aggregation 30
6.2.2 EV-associated proteoglycans have minor impact on Aβ(1-42) aggregation 31
6.2.3 Lipids can delay and accelerate Aβ(1-42) aggregation 32
6.3 EV-Aβ(1-42) crosstalk affects EV properties, Aβ(1-42) aggregation and accumulation 36
7. Concluding Remarks 42
8. Acknowledgements 44
9. References 45

1. Introduction

Alzheimer's disease (AD) accounts for ~70 % of dementia cases and is the 7th leading cause of death worldwide [1]. More than 55 million people worldwide were reported to live with dementia in 2021, and this number is expected to rise to almost 80 million by 2030, representing a growing global health challenge as the ageing population increases [2]. A central pathological hallmark of AD is the presence of extracellular plaque deposits that contain highly ordered, β-sheet rich protein assemblies known as amyloid fibrils [3]. These fibrils form via self-assembly of the amyloid-β (Aβ) peptide.

Our understanding of AD has advanced markedly since it was first described by Alois Alzheimer over a century ago [4], yet our current knowledge of the mechanisms that initiate and drive disease progression is incomplete. Aβ fibrillar structures were identified as major components of plaque deposits around 40 years ago [5], and in the early 1990s Hardy and Higgins formalized the amyloid cascade hypothesis, proposing that Aβ accumulation is an initiating event that drives downstream pathology in AD [6]. This hypothesis has shaped the field for decades and motivated extensive research to define and, on a molecular level understand, the role of Aβ in AD pathology. Over time it was increasingly realized that plaque burden correlated rather poorly with cognitive decline and evidence emerged that soluble Aβ oligomers are highly neurotoxic and therefore may represent the most disease-driving species [7-9]. This led to a refinement of the amyloid cascade hypothesis and a marked shift in research focus towards characterising and understanding these species.

Today, it is increasingly common to study Aβ oligomers and fibrils in consort, instead of adopting a singular view. These developments have also increased the need for research tools that can be used to accurately explore and mechanistically explain Aβ self-assembly. Over the last decade, significant advances in the field of biophysics have resulted in a framework that enables the identification and quantitative description of microscopic steps involved in *in vitro* Aβ aggregation based on the analysis of carefully monitored kinetics [10, 11]. This includes the formation of smaller Aβ species thought to be particularly neurotoxic [10]. Such studies have revealed that once a critical concentration of Aβ fibrils is reached, Aβ aggregation proceeds with autocatalytic amplification via a secondary nucleation mechanism by which new monomers nucleate at the surface of existing fibrils. This mechanism is, in fact, the major source of Aβ aggregates, including smaller, more toxic, Aβ assemblies. More recently, advances in cryo-electron microscopy (cryo-EM) have revolutionized amyloid structure research, now making it possible to gain insight into amyloid architectures with near-atomic resolution [12]. Cryo-EM has, for example, made it possible to compare *in vitro* assembled fibrils with fibrils extracted from postmortem human brain tissue. These advances are about to reshape hypothesis-building in amyloid research by allowing more direct links between amyloid structure and function to be tested.

Despite these massive advances, AD remains an incurable disease. A significant problem is that we still do not understand what triggers the initial formation and accumulation of Aβ aggregates, or how to effectively slow down or prevent their formation. In recent years, antibody therapies targeting Aβ aggregates [13] have gained clinical approval based on their ability to moderately slow down disease progression in early-stage AD [14]. This represents a significant step forward for a field that has long lacked success in the form of disease-modifying treatments. Moreover, it provides clinical confirmation for the amyloid cascade hypothesis, and modified versions thereof, by demonstrating that reducing Aβ accumulation can slow cognitive decline. However, their use remains limited by hitherto modest clinical benefit in combination with high costs. Also, it should be remembered that the antibodies that underlie current clinical success were developed almost 20

years ago [15], prior to the advancement of kinetic analyses and detailed amyloid structure, suggesting that with increasing knowledge, their design could also improve.

AD is a multifaceted disease in which multiple factors likely contribute to neurodegeneration. Although the role of Aβ as a driver of AD pathology is widely supported by pathological, genetic, biochemical and, now also pharmacological, evidence, the factors that initiate Aβ aggregation and drive accumulation are still not fully understood. It is likely that perturbances in combinations of cellular pathways and molecules contribute to establish an imbalance between Aβ production, clearance, trafficking, and accumulation. Probing how different biological modifiers contribute to Aβ aggregation and accumulation is therefore important to increase fundamental understanding of disease pathology as well as for the future development of effective therapeutics.

The aim of my thesis work has been to increase understanding of how extracellular vesicles (EVs), which are nanosized membrane-enclosed particles released by cells, modulate the aggregation and intraneuronal accumulation of the disease-prone and highly neurotoxic 42-amino acid Aβ(1-42) variant. In **paper I**, I showed that EVs slow down Aβ(1-42) aggregation kinetics *in vitro* by interfering with the elongation reaction step, resulting in the formation of significantly shorter fibrils, which could possibly have altered neurotoxicity. P**apers I-II** show that this effect is shared by EVs from different cell origins, suggesting that common EV properties, rather than specific biomolecules, underlie the inhibition. In **papers II** and **III**, I further investigated this modulatory role by identifying how key classes of EV surface components contribute to the aggregation-modulatory effect. In **paper II**, I showed that enzymatic removal of surface-associated proteins increases the inhibitory effect of EVs on Aβ(1-42) aggregation, suggesting that the EV lipid bilayer exerts a strong inhibitory influence that may be somewhat masked by proteins. In **paper III**, the lipid effect was further studied using synthetic lipid vesicles and this work pointed out the importance of lipid raft-like microdomains and ganglioside clustering on Aβ(1-42) aggregation. Finally, in **paper IV**, I investigated Aβ(1-42)-EV crosstalk and showed that endolysosomal accumulation of Aβ(1-42) increases EV secretion and alters EV properties. Furthermore, I found that EVs from Aβ(1-42) pre-treated cells, in turn, exert stronger inhibitory effect on Aβ(1-42) aggregation whilst also increasing Aβ(1-42) cellular accumulation, suggesting a strong bidirectional relationship.

Thesis outline

This thesis begins with an overview of the research area and introduces the rationale for investigating Aβ-EV interactions in AD. Chapters 2-4 provide scientific background, covering protein folding and misfolding, Alzheimer's disease, Aβ, and its aggregation, EV biogenesis and composition, and current knowledge on the role of EVs in Aβ pathology. Chapter 5 describes the methods used throughout this thesis and their applications. Last, in chapter 6, I summarize and discuss the main findings from my work (**paper I-IV**).

2. Proteins and Amyloid Fibrils

2.1. **Protein Folding and Misfolding**

Proteins constitute a diverse class of biomolecules that carry out essentially all vital functions that are needed in cells of living organisms. The final three-dimensional structure (fold, native state) of a protein is determined by its primary sequence. Folding to adopt this state typically occurs spontaneously due to that the native conformation corresponds to the lowest free energy that the single amino acid sequence can adopt, as depicted in the left-hand part of the energy landscape in Figure 1. Forces and interactions such as the hydrophobic effect, intramolecular hydrogen bonds, van der Waals forces and electrostatic forces contribute to the stability of a protein in its native state. There is a great number of possible conformations a protein can adopt, yet the protein folding process to its native state takes, in many cases, only between microseconds to seconds, suggesting that polypeptides fold via preferred pathways in their search for the native state. However, proteins can also fail to achieve or maintain their native fold and instead misfold into inactive or dysfunctional forms, some of which even gain toxic functions [16]. One possible outcome of protein misfolding is the formation of highly organized protein aggregates enriched in β-sheet structure. These are known as amyloid fibrils [17] and can be highly thermodynamically stable, with a lower free-energy minimum than their native folded state (Figure 1). These aggregation processes typically proceed through smaller assemblies known as oligomers, which can be either off-pathway species or on-pathway intermediates towards the formation of larger amyloid fibrils [17]. While cells normally counteract misfolding through a variety of proteostasis mechanisms, including the actions of molecular chaperones which help proteins fold into their native state [18], persistent misfolding and resulting amyloid formation are implicated in the pathology of many human diseases including severe conditions such as Alzheimer's disease (AD). To date, there are approximately 40 amyloid forming proteins that have been linked to human disease [19].

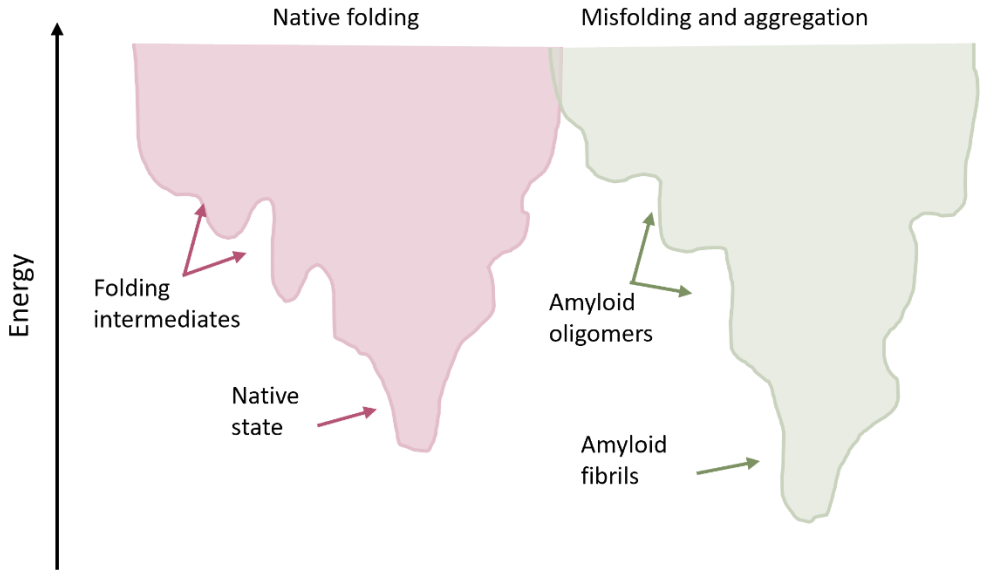

Figure 1. A simplified illustration of the energy landscape of protein folding, including the cross-over to misfolding and aggregation.

2.2 **Amyloid Fibrils**

The term amyloid, meaning "starch-like", was first introduced in the 1850s by Rudolph Virchow as a description of *in vivo* amyloid deposits, and this name persists today, even though amyloid was subsequently shown to consist of proteins rather than carbohydrates [20]. Today much more is known about the structure of fibrils of the type that exist in such deposits; amyloid fibrils are unbranched, typically twisted self-assembled protein polymers, with a characteristic cross-β structure in which the β-strands run perpendicular to the fibril axis and assemble into β-sheets that extend along the length of the fibril (Figure 2) [21]. X-ray diffraction analyses of amyloid fibrils have revealed that these β-sheet rich fibrils display two hallmark reflections at ~ 4.7 Å, corresponding to the distance between β-strands in a β-sheet, and at 10-11 Å, corresponding to the distance between β-sheets (Figure 2) [22-24]. These repeating structures align to form protofilaments, of which each protofilament is approximately 2-7 nm in diameter. The protofilaments twist around each other to form a mature fibril with a diameter of 5-13 nm [25, 26]. Extensive hydrogen bonding of β-sheets along the filament axis, together with tight inter-sheet packing, contributes to the high stability and low solubility of amyloids. Although the cross-β arrangement is a common feature in amyloid fibrils, a single protein sequence can adopt multiple distinct fibril structures; this phenomenon is referred to as amyloid polymorphism and can arise from differences in protofilament number, protofilament packing/interfaces, or monomer folding within the fibril core [27]. In recent years, many amyloid fibril structures have been resolved by the use of cryo-electron microscopy (cryo-EM) [12], which can resolve monomer fold, protofilament number and protofilament interfaces at near-atomic detail. This has provided significant new insight into the architecture of amyloid fibrils, including fibrils extracted from postmortem human brain tissue and fibrils assembled under various *in vitro* conditions, highlighting the diversity and complexity of amyloid folds.

The Alzheimer's disease (AD) related amyloid-β (Aβ) peptide, which is at focus in this thesis, has been found to form a variety of amyloid fibril folds that differ in protofilament numbers, twisting of the fibrils, and protofilament packing and interactions [28-30]. Cryo-EM of brain-derived Aβ(1-40) and Aβ(1-42), which are the two most common Aβ variants in AD [31], suggest that *in vivo* Aβ(1-40) fibrils are predominantly built from pairs of identical protofilaments, but fibrils consisting of four or six protofilaments are also present [29]. For brain-derived Aβ(1-42), two major fibril structures have been described; both composed of two protofilaments but differing in protofilament packing, where type I appears predominant in sporadic AD and type II in familial AD [32]. In Aβ(1-42) carrying the E22G arctic mutation which causes dominantly inherited AD, most fibrils consist of two pairs of non-identical protofilaments [30]. Interestingly, despite that Aβ fibrils can adopt all these distinct folds, they are all consistently associated with AD.

Understanding the amyloid fold, and even more so how amyloid fibrils form, is important for future development of strategies to prevent or modulate amyloid pathology. Amyloid aggregation reactions and how they can be perturbed by biological modulators is also a central part of this thesis. The next section outlines general principles of amyloid aggregation, while a detailed description of the aggregation mechanism of the Aβ(1-42) peptide is given in chapter 3.2.

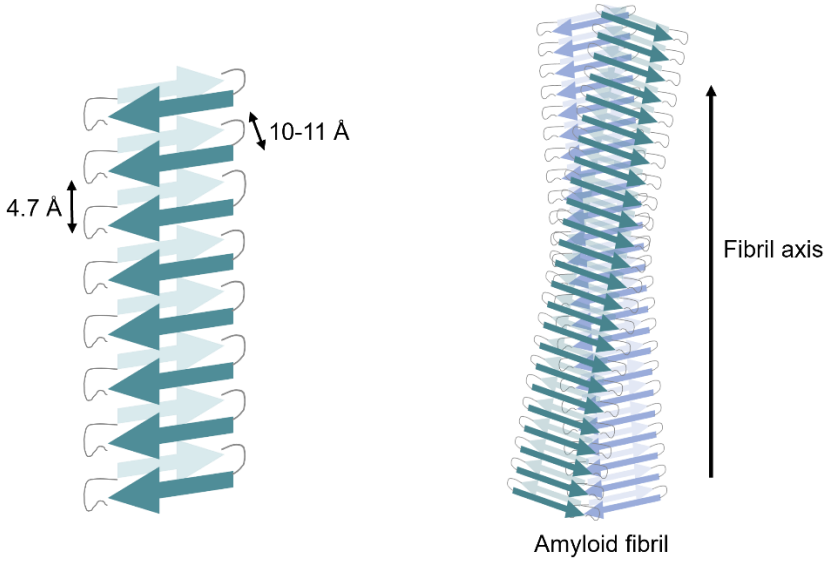

Figure 2. Illustration of an amyloid fibril structure. The left image depicts the β-sheet structure arrangement within the amyloid fibril with the β-strand and β-sheet spacing. The right image illustrates an amyloid fibril arrangement with two protofilaments where each consists of two β-sheets.

2.3 Amyloid Aggregation

As already touched upon, amyloid aggregation occurs when the fibril state is thermodynamically favoured. This most commonly occurs under supersaturated conditions where the monomer concentration exceeds the effective solubility of the protein. However, reaching the fibrillar state requires overcoming kinetic barriers, and the rates can be influenced by intrinsic factors (e.g. sequence-dependent aggregation propensity [33], point-mutations [34], and post-translational modifications [35]) and extrinsic modulators (e.g. pH and temperature) [36, 37]. Extrinsic modulators can also include other components that are present in the protein's biological milieu, for example lipids [38-40], metal ions [41], chaperones [42], and extracellular vesicles (EVs) [43-45], which can change aggregation rates and alter aggregation mechanisms. The role of EVs in Aβ aggregation is the central topic of this thesis.

The kinetic barriers in amyloid formation reflect distinct microscopic steps in the aggregation processes; these steps are schematically depicted in Figure 3. The conversion of partially or completely disordered monomers to nuclei which can initiate further fibril growth is called primary nucleation. This is the slowest step in the aggregation process and consequently associated with the lowest rate constant [10, 46]. Once formed, these primary nuclei can continue to grow by the addition of monomers to their ends, a process which is called elongation and has a lower energy barrier than primary nucleation and thus a higher rate constant. Fragmentation is a process in which fibrils break into smaller pieces, resulting in an increase in available fibril ends that can support elongation. Another critically important mechanism in the formation of amyloid fibrils is the formation of new nuclei on existing fibrils, by which the fibril surface acts as a catalyst. This is called secondary nucleation [10] and is associated with a very low energy barrier and a high rate constant, leading to a rapid multiplication of aggregates.

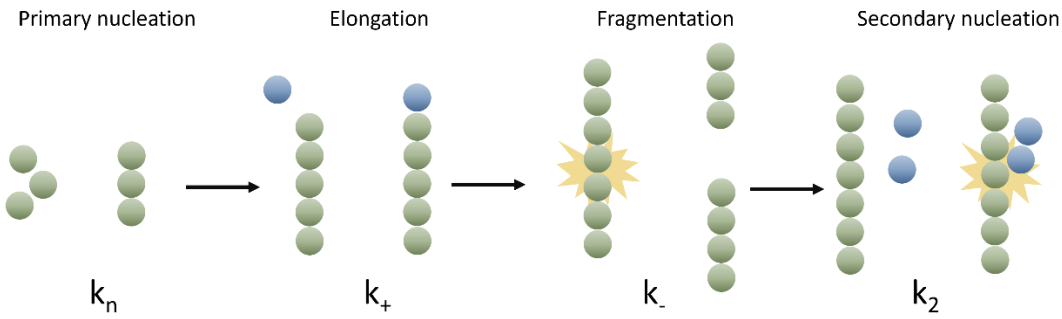

Figure 3. Illustration of the different mechanistic steps involved in amyloid formation, including primary nucleation, elongation, fragmentation and secondary nucleation.

Amyloid fibril formation kinetics typically follow a sigmoidal trajectory (Figure 4) consisting of three phases. The first phase, the lag phase, is dominated by primary nucleation, during which fibril growth is not yet observable. During this phase oligomeric species can also form, and these are often innately unstable [47, 48]. The subsequent growth phase is characterized by rapid fibril formation, occurring largely due to secondary processes which drive the formation of new aggregates, including oligomers. Finally, if the concentration of monomers in the sample is limited, a stationary phase, or plateau, is reached, in which fibrils and monomers exist in equilibrium [49].

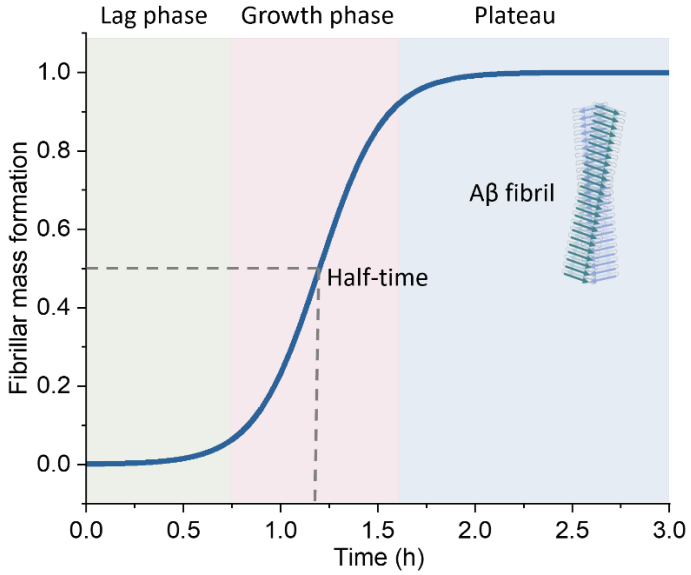

Figure 4. Illustration of Aβ(1-42) fibril formation kinetics showing a sigmoidal aggregation curve with lag, growth, and stationary (plateau) phases. The half-time is indicated and represents the time required to reach 50% of the maximal fibril mass fraction.

Amyloid aggregation kinetics has been described mathematically by the master equation below (Equation 1), which can be used to quantify the different microscopic processes and determine their individual rates (e.g. to understand the molecular mechanisms of the aggregation process):

$$\frac{M(t)}{M_\infty} = 1 - \left(\frac{B_+ + C_+}{B_+ + C_+ e^{\kappa t}} * \frac{B_- + C_+ e^{\kappa t}}{B_- + C_+}\right)^{\frac{k_\infty^2}{\kappa k_\infty}} e^{-k_\infty t} \quad (1)$$

where

$$\lambda = \sqrt{2k_+ k_n m(0)^{n_c}}$$

$$\kappa = \sqrt{2k_+ k_2 m(0)^{n_2+1}}$$

$$B_\pm = (k_\infty \pm k'_\infty)/(2\kappa)$$

$$C_\pm = \pm\lambda^2/(2\kappa^2)$$

$$k_\infty = \sqrt{\frac{2\kappa^2}{n_2(n_2+1)} + \frac{2\lambda^2}{n_c}}$$

$$k'_\infty = \sqrt{k_\infty^2 - 4C_+ C_- \kappa^2}$$

This mathematical model, and extensions of it, can be fitted to experimental data to estimate individual rate constants. One can thus learn how changes in experimental conditions, such as for example the presence of certain extrinsic modulators, affect not only the overall aggregation rate, but also the aggregation mechanism. An online platform called AmyloFit [11] has been developed to facilitate these types of fittings. Model fittings to experimental data have been used extensively in this thesis to understand the effect of EVs and specific EV components (mainly lipids) on Aβ aggregation kinetics, and the modelling procedures used are further explained in chapters 3.2 and 5.2.1.

3. Alzheimer's Disease

Alzheimer's disease (AD) was first described in 1906 by Alois Alzheimer; his findings published in 1907 describing what at that time was called presenile dementia [4]. Shortly after, the disease became known as Alzheimer's disease, and it is today recognized as a severe and devastating neurodegenerative disorder affecting millions of individuals and their families worldwide [50]. Both familial and sporadic forms of AD exist. While familial AD progresses faster and often onsets in individuals with lower age (typically < 65 years), it only accounts for 5% of all AD cases [51]. Familial AD is typically an autosomal dominant disorder and is most commonly caused by pathogenic mutations of specific genes such as the presenilin 1 and presenilin 2 genes and the amyloid precursor protein gene. Sporadic AD, also called late-onset AD, typically develops later in life but there are certain known risk factors that can lower the age of onset. These include genetics, lifestyle, and environmental factors [52, 53].

Despite massive efforts to understand and treat AD, effective therapies remain extremely limited. Developments over the last few years, have, however, marked a turning point with the approval of Aβ-targeting monoclonal antibodies for treatment of early symptomatic AD, resulting in a slowed cognitive decline in clinical trials [14, 54]. At the same time, AD is viewed as a multifaceted disease in which parallel pathological processes develop and crosstalk. In addition to protein aggregation, these include synaptic dysfunction, neuroinflammation, vascular changes, metabolic stress, and intracellular trafficking and protein clearance dysfunctions. It is likely that the efficacy of AD treatments could be improved if we gain better understanding of all these dysfunctions, as well as their interrelations. AD targets the hippocampus and the cerebral cortex of the brain, leading to the degeneration of neurons [55]. Symptoms of the disease include memory loss, disorientation, language difficulties and behavioural changes [3, 56]. As the disease progresses and brain function continues to decline, the risk of secondary conditions such as pneumonia and sepsis increases, making AD ultimately fatal. Key pathological hallmarks of the disease include senile plaques deposited extracellularly in brain tissue and intracellular neurofibrillary tangles [3]. The amyloid-β (Aβ) peptide is the main component found in plaques while neurofibrillary tangles consist of hyperphosphorylated tau. Both Aβ and tau form β-sheet rich amyloid structures and are considered key pathological components in AD.

The Aβ peptide and its aggregation and accumulation are central in this thesis and the Aβ structure, aggregation and pathology are further described in the next sections.

3.1 The Aβ Peptide

The Aβ peptide is a cleavage product of the transmembrane amyloid precursor protein (APP) (Figure 5). The amyloidogenic processing of APP occurs (mainly) in the endosomal pathway in neurons [57], starting with cleavage by the membrane-associated β-amyloid cleaving enzyme BACE1, also called β-secretase. The acidic environment in endosomes is optimal for BACE1 enzyme activity and BACE1 cleavage results in the release of a soluble N-terminal ectodomain (sAPPβ) and a 99 amino acid long membrane-embedded C-terminal fragment (CTFβ) [58]. This first cleavage is followed by a second cleavage of CTFβ by the γ-secretase complex composed of four subunits (presenilin 1 or 2, (PSEN1/PSEN2), nicastrin, presenilin enhancer 2 (PEN-2) and anterior pharynx-defective 1 (APH-1)) [59], generating ~ 4 kDa Aβ peptide. Depending on the exact site of cleavage by γ-secretase, different isoforms of Aβ (typically 37 to 49 amino acid residues) are generated [60]. The most abundant Aβ isoforms are Aβ40 (80-90%) and Aβ42 (5-

10%), the latter of which is more hydrophobic, has higher propensity to aggregate into amyloid fibrils and typically also displays more neurotoxicity [31].

APP can also be cleaved in a non-amyloidogenic pathway by the α-secretase protease complex (metalloprotease enzymes), followed by cleavage by the γ-secretase complex into the more benign p3 peptide. Under basal conditions, most APP is processed via α-secretase, whereas β-secretase cleavage represents a smaller fraction. Accordingly, β-secretase is often considered the rate limiting step in the amyloidogenic processing of APP [60].

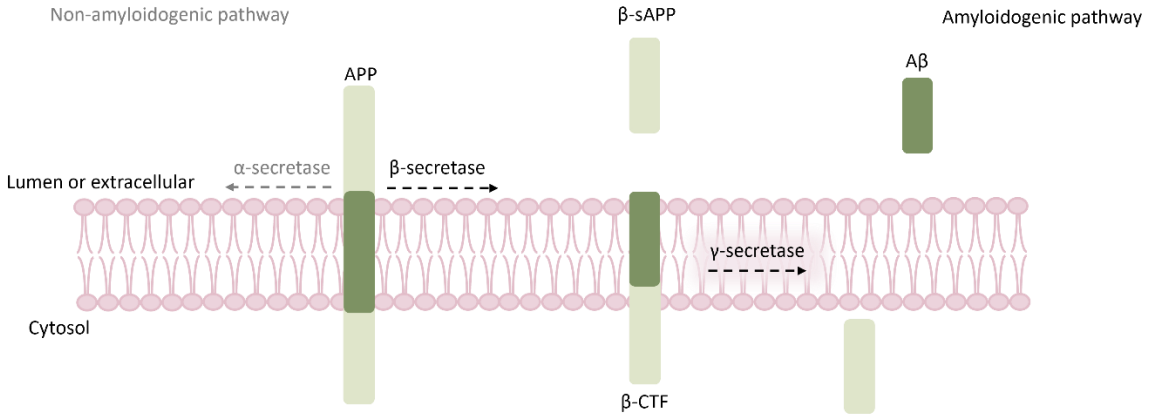

Figure 5. Schematic illustration Aβ formation and release through the amyloidogenic cleavage of APP via β- and γ-secretases. APP can also be cleaved through the non-amyloidogenic pathway initiated by α-secretase.

The primary amino acid sequence of Aβ(1-42), which is the variant studied in this thesis, is shown in Figure 6. In its native form, Aβ(1-42) is monomeric and unstructured. It has a predominantly hydrophilic N-terminus (residues 1-16) which also contains key sites for metal-ion binding [61], followed by a central hydrophobic region and a central polar region, and a more hydrophobic C-terminal region with enrichment of non-polar residues (30-42) [62]. The central hydrophobic region, together with a region of the C-terminus plays a critical role in aggregation of the peptide [63] and the fibril core is enriched in hydrophobic segments that repeatedly appear as β-strand elements consisting of these two segments. Several disease-associated Aβ mutations cluster in the 21-23 region, such as the Arctic E22G, Dutch E22Q,Italian E22K, and Iowan D23N mutations [64], and many of these lead to accelerated Aβ aggregation, highlighting that even small sequence changes near this central segment can alter fibril formation and polymorphism.

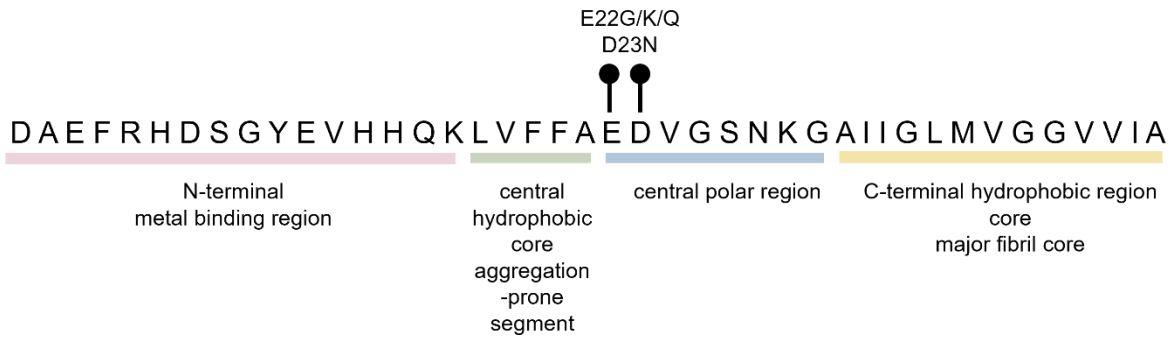

Figure 6. Aβ(1-42) primary sequence with annotated sequence regions and selected common familial variants.

3.2 Aβ Aggregation

The Aβ peptide is unfolded in its monomeric state but has a high propensity to self-assemble into amyloid fibrils [65]. Since the Aβ(1-42) variant has been studied in this thesis, this next part focuses on what is known about the aggregation kinetics and aggregation mechanisms of this isoform.

Aβ(1-42) fibril formation follows the microscopic reaction step framework introduced in chapter 2.3 and involves primary nucleation, elongation, and secondary nucleation. The aggregation of Aβ(1-42) is characterized by a rapid autocatalytic amplification of fibrils once a critical seed concentration has formed, because its fibril surfaces catalyse the generation of new nuclei via secondary nucleation [10, 66]. As fibril mass increases, the available surface area increases, which further accelerates the production of new aggregates and drives the steep rise during the growth phase of Aβ(1-42) fibril formation. The reaction then approaches a plateau as soluble monomer is depleted towards its equilibrium concentration; typically more than 90% of monomers are converted into fibrils in *in vitro* aggregation reactions [67]. Importantly, secondary nucleation is thought to be a major source also of Aβ oligomeric species [10, 68] which are smaller soluble multimers that may not be elongation-competent in their current molecular state but are strongly associated with neurotoxicity [8, 9, 69]. These species are considered important in the development of Aβ-induced neuropathology and are therefore further described in chapter 3.3. Therapeutic intervention strategies often aim to reduce oligomer exposure in the brain. This does not necessarily have to entail complete elimination of fibril formation; instead a key strategy could be to selectively suppress the microscopic processes that generate toxic oligomeric intermediates, e.g. secondary nucleation [70].

The aggregation of Aβ into amyloid fibrils is affected by a variety of intrinsic and extrinsic modulators, which can influence both overall amyloid formation propensity and resulting fibril morphology, but also shift the balance between the microscopic steps that drive the reaction. Intrinsic modulators include for example disease-linked genetic changes in APP and PSEN/PSEN2 which alters the Aβ primary sequence or affects which Aβ isoforms are produced [64, 71]. Post-translational modifications are another intrinsic modulator that can affect Aβ charge, hydrophobicity, metal binding and intermolecular contacts [72, 73], leading to changes in aggregation [74]. Extrinsic modulators include solution conditions such as pH, ionic strength, and temperature, as mentioned earlier, but also biological components. For example, molecular chaperones can bind to Aβ and affect its aggregation [75].

Lipid membranes are also important modulators. Gangliosides such as GM1 [39, 76] together with the lipids cholesterol and sphingomyelin [39, 77] can form lipid raft-like domains that sequester or concentrate Aβ at the membrane surface, thereby accelerating or inhibiting Aβ aggregation [78].

In addition, metal ions [41] and heparan sulfate proteoglycans [79] can affect the self-assembly of Aβ aggregates. A central theme of this thesis is whether extracellular vesicles (EVs), which present a lipid bilayer with associated proteins and glycans and are omnipresent in the interstitial fluid surrounding neurons where Aβ is located, can function as modulators of Aβ aggregation. EVs as biological entities are introduced in chapter 4 and current knowledge of their role in Aβ pathology is described in chapter 4.3.

3.3 Aβ Pathology

Even though Aβ is best known for its pathological role in AD, the peptide is produced throughout life and in both diseased and non-diseased individuals [80]. A widely accepted view is that AD pathology emerges when Aβ production, trafficking, and clearance become imbalanced, and that this leads to accumulation of soluble oligomeric species and, later, larger aggregates, that drive neurotoxicity, plaque deposition, and disease progression [81]. The amyloid cascade hypothesis was first introduced in 1992 and proposed, in its original version, that Aβ plaque deposition was the main pathogenic cause of AD [6]. This view has since been modified, in part because plaque burden correlates poorly with cognitive decline [82] and the hypothesis now includes soluble (oligomeric) Aβ species which can induce synaptic dysfunction and cognitive deficits [69].

Many studies suggest that oligomeric assemblies are more cytotoxic than the fibrillar Aβ that is deposited into plaques [7, 9, 69]. Moreover, it has been suggested that oligomeric assemblies and other soluble amyloid aggregates will induce cognitive deficits even prior to the emergence of plaque deposits [9]. At the same time, Aβ has been shown to exist in many different assembly types and fibrillar species also contribute to toxicity, for example by providing catalytic surfaces that generate new species, including oligomers, via seeding and secondary nucleation, as described in chapter 3.2. Mapping protein aggregation pathways and exploring how amyloid formation is regulated by biological components, as is the focus of this thesis, is one important path towards understanding how this imbalance is created, which in turn is crucial for our molecular understanding of Aβ pathology and ability of developing functional therapies in the future.

Multiple, and often overlapping, mechanisms have been proposed to explain Aβ toxicity. Aβ can disrupt synaptic dysfunction through receptor-associated mechanisms that perturb glutamate signalling and calcium homeostasis, and oligomers may additionally compromise membrane activity, further promoting pathological calcium influx and impaired plasticity [83, 84]. Aβ oligomers have been implicated in mitochondrial dysfunction, including altered mitochondrial quantity and quality, which promotes oxidative damage [85, 86]. Microglia initially respond by clearing Aβ, but increased accumulation of Aβ in microglia can shift them towards overactivated states. This promotes neuroinflammation, oxidative stress, and neuronal damage [87]. Oxidative stress is a recurring component revolving Aβ toxicity, and Aβ can promote reactive oxygen species and oxidative damage, including lipid and protein oxidation [88, 89]. Finally, Aβ accumulation promotes hyperphosphorylation of the AD-related tau protein, enhancing the toxic effect of phosphorylated tau on synapses [83].

Accumulating evidence suggests that Aβ peptides are internalized by neurons where they accumulate in, and potentially jam, their endolysosomal systems [90, 91]. Enlarged endosomes are, in fact, one of the earliest observable pathological alterations in the AD brain [92]. Such endolysosomal dysfunction is an important contributor to the imbalance of Aβ production and clearance. Aβ that accumulates in late endosomes, including multivesicular bodies (MVBs), can be secreted in association with exosomes when MVBs fuse with the plasma membrane and release their intraluminal vesicles as exosomes (a subtype of EVs) [93]. Moreover, if lysosomal degradation is impaired, trafficking may be shifted from clearance toward secretion [94], potentially increasing the exosome-associated release of Aβ and thereby contributing to the spread of Aβ pathology. The crosstalk between Aβ and EVs is central to this thesis and how Aβ accumulation intersects with EV biogenesis and release is a focus of **paper IV**.

4 Extracellular Vesicles

As mentioned earlier in the thesis, crosstalk between Aβ and EVs has been suggested in AD. This chapter first gives an overview of what EVs are, how they are generated and their compositions as well as of their cell uptake (partly explaining how they function) and finally outlines current knowledge of the role of EVs in AD, focusing specifically on the intersection with Aβ pathology.

EVs are nanosized membrane-enclosed vesicles (Figure 8) released by all cells into their surrounding microenvironment. They are increasingly recognised as important mediators of intercellular communication, capable of transporting a diverse range of cargos including proteins, lipids, nucleic acids and metabolites between cells, even mediating communication between organs [95, 96]. Observations of vesicle-like structures released from cells trace back to as early as the 1950-1970s, describing particles that today would likely be described as EVs [97]. Initially, such vesicles were viewed as cellular debris or as a route for disposal of membrane proteins and other components considered as cellular waste. A conceptual shift occurred around the 1980s, when studies showed that intraluminal vesicles can be released from cells, eventually leading to the term "exosome" to describe EVs that shed from the cell surface. Subsequent work began to define physical and biochemical characteristics of EVs and showed that EVs can carry molecules of interest, suggesting that they can be explored as biomarkers and in future therapeutic applications [98]. These early findings led to a rapid increase in the interest in EV biology around the turn of the millennium. The EV proteome [99] and lipidome [100] was further explored, and the interest in EV function grew as reports on the role of EVs in the immune system and in cancer increased. Furthermore, studies started reporting on functional effects of EVs in vivo [101].

Today EVs are acknowledged for their diverse roles in biological systems and their roles in neurodegenerative disease are also being investigated, with EVs implicated in the spread and modulation of pathogenic proteins such as Aβ [44, 102]. EVs are now being explored in numerous applications, including biomarker discovery, therapeutic development, and targeted drug delivery [103].

4.1 EV Biogenesis and Composition

EVs are highly heterogenous both with respect to physical parameters such as size and biochemical parameters such as molecular composition. In literature, EVs are broadly characterized into the two subcategories exosomes and ectosomes [104]. Exosomes originate from the endosomal system where they first form by invagination of the limiting membrane of late endosomal structures called multivesicular bodies (MVBs). This results in so-called intraluminal vesicles (ILVs) which can either be degraded through fusion of the MVBs with lysosomes, or released into the extracellular space as exosomes upon MVB-fusion with the plasma membrane [105]. Ectosomes, on the other hand, are generated from the outward budding of the plasma membrane. The size of EVs can range between approximately 50 – 1000 nm [106]. Because exosomes originate as ILVs, they are typically described to be in the ILV size range of 50-150 nm [107], whereas ectosomes can span a wider size range. There is a substantial size overlap, making it impossible to separate exosomes and ectosomes. Two major EV biogenesis pathways have been identified. They are either dependent or independent of the endosomal sorting complex required for transport (ESCRT). The ESCRT machinery, initiated by the recognition of ubiquitinated proteins on the endosomal or cell surface membrane, is composed of several protein complexes, which, among other things, function to facilitate MVB formation, vesicle budding and sorting of protein cargo. While ectosomes are not formed in the endosomal pathway, certain ESCRT subunits and

tetraspanins also play a role in ectosome budding and cargo sorting. The ESCRT-independent pathway involves sorting cargo within the endosomal membrane dependent on raft-based microdomains containing ceramides, highlighting the importance of lipids in EV biogenesis [108].

As mentioned, EVs carry different cargoes, both within their lumen and on their surfaces (Figure 7). The EV lumen contains cargo derived from the parental cell, while the EV surface is, in part, a reflection of the parent cell membrane. The EV surface is the first point of contact with recipient cells and other extracellular moieties, and is thus important in mediating recognition, uptake, and signalling [109]. In this thesis, I have studied EV-Aβ interactions with a particular focus on the EV surface and its role in modulating Aβ aggregation, and the following section will therefore outline key aspects of EV surface composition.

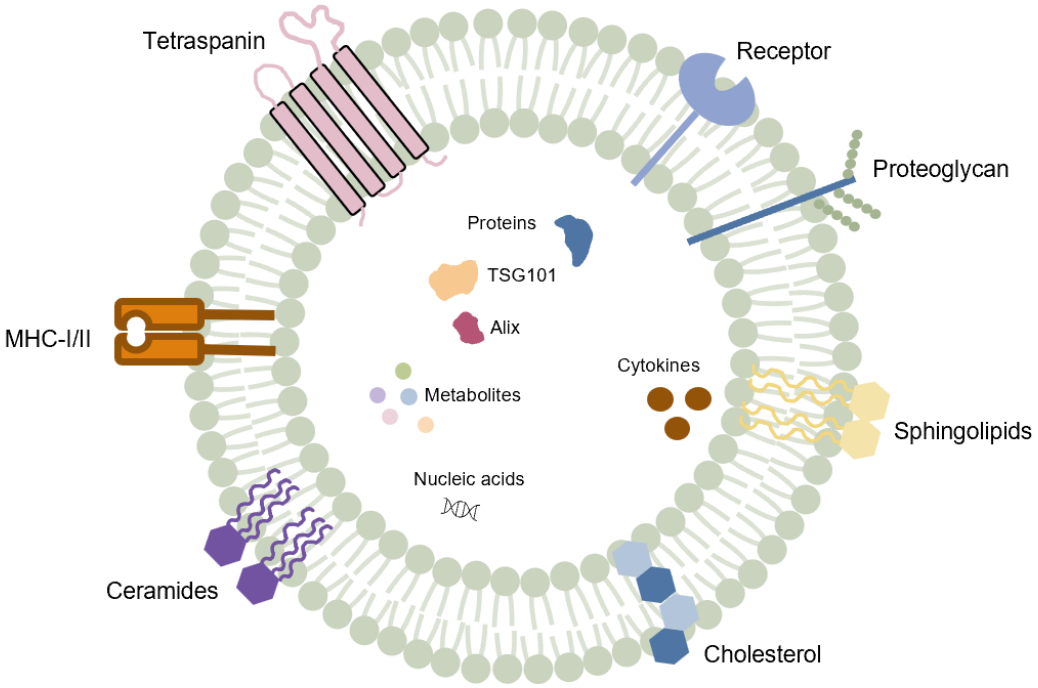

Figure 7. Illustration of an EV and its molecular cargo, including lipids, nucleic acids, proteins, and metabolites located on the membrane or in the lumen.

Large-scale proteomics studies have yielded online databases of catalogued EV-associated proteins, both surface-associated and luminal proteins. Although the variety is huge, certain EV surface proteins are detected in a majority of, if not all, EV samples. These include for example tetraspanins such as CD63, CD81, and CD9, which are thought to contribute to the organization of membrane microdomains, facilitate cargo sorting and thus both regulate EV biogenesis and mediate intercellular communication [110] even though their exact roles in these processes remain incompletely understood [111]. EVs also display surface proteins that reflect their cellular origin and specialized functions. For example, tumour-derived EVs can carry molecules promoting immune escape [112] or pro-angiogenic factors that support tumour progression [113], dendritic cell-derived EVs can contain molecules involved in immune activation [101], and stem cell-derived EVs can deliver components promoting tissue repair [114], supporting the idea that they can take on special functions.

Lipidomic profiling has substantially advanced our understanding of EV membranes. As in cells, phospholipids are the major lipid class in EV membranes and include phosphatidylcholines (PC) and phosphatidylethanolamines (PE), and to a lesser extent also phosphatidylserines (PE) and phosphatidylinositol (PI), which help maintain membrane fluidity and stability [109, 115]. EVs are typically enriched in sphingolipids, including sphingomyelin which is involved in the formation of lipid rafts [116] and thus the compartmentalization of membrane processes. EVs are also enriched in cholesterol which is a major modulator of membrane stiffness. Cholesterol-rich lipid rafts can influence EV biogenesis and function [117, 118]. Lipid membranes are generally asymmetric and this applies to EV membranes as well, where sphingomyelin and PC are typically located in the outer leaflet while PE and PI are found on the inner leaflet [115]. The EV lipid composition reflects their cellular origin and different EV types can thus have unique lipid compositions [119]. The lipid composition of EVs can also reflect the status of the cell, and lipidomic differences in EVs from AD vs control human plasma samples have been detected [120].

EVs can further be functionalised by post-translational protein glycosylation which contributes to the net negative EV surface charge. The EV glycocalyx consists of glycoproteins, proteoglycans bearing glycosaminoglycan chains (e.g. heparan sulfate on syndecans and glypicans), and glycolipids [109]. These sugar moieties are important in cell-cell interactions and cellular uptake, and these properties are translated to EV interactions and uptake of recipient cells as well [109, 121].

4.2 Cellular Uptake of Extracellular Vesicles

Once EVs have been released from cells, they can travel short and long distances within and across organs. EVs have consequently been detected in multiple biofluids including blood, cerebrospinal fluid, interstitial fluid, saliva, and urine [103]. EVs can cross the blood-brain barrier [122, 123] and they can move through tissue, although the exact mechanisms for this are still not understood [124]. For EVs to exert their function and deliver their cargo, they must dock to and/or be internalized by recipient cells. The understanding of these processes is incomplete but examples include integrin/tetraspanin-mediated interactions, glycan-dependent binding (e.g., to HSPGs), and phosphatidylserine-dependent recognition [121, 125, 126]. Cell uptake of EVs occurs via endocytosis, including receptor-mediated mechanisms [127, 128], macropinocytosis [129], and phagocytosis [130, 131].

Once internalized, EVs are trafficked through the endosomal pathway. They can either be recycled back to the plasma membrane [132], or traffic via late endosomes to lysosomes for degradation. During endosomal processing, EVs can, under some circumstances, fuse with endosomal membranes and release their cargo into the cytosol [133] but the efficiency of this process is likely very low.

4.3 Extracellular Vesicles and Aβ Pathology

EVs have been suggested as potential modulators of disease pathology across a broad spectrum of conditions, including AD [44, 93, 134, 135] and other neurodegenerative disorders [136]. In recent years, EVs have been increasingly explored as biomarkers for AD and as putative therapeutics [137, 138]. In preclinical AD rodent models, EV treatments have been reported to improve cognitive performance, reduce Aβ plaque burden, and attenuate neuroinflammation and oxidative stress [139-142]. Conversely, EVs have also been shown to function as carriers of Aβ

and APP cleavage products [143], suggesting that they may contribute to cell-cell transmission and disease progression. At the start of my thesis work, direct EV- Aβ interactions remained, however, poorly explored. Understanding such interactions is important from a fundamental perspective, but determining the specific conditions under which EVs modulate Aβ pathology in respectively beneficial and detrimental ways, and connecting them to specific EV molecular characteristics, is also critical for the future use of EVs as biomarkers or in therapeutic applications.

My thesis investigates Aβ-EVs crosstalk, focusing on the direct interaction perspective and on the aggregation aspect of Aβ pathology. There are two conspicuous biological intersections between Aβ and EVs. First, both are produced in the endolysosomal system, where Aβ furthermore accumulates in early stages of AD. Second, they can both be secreted and thus meet in interstitial locations of the brain where Aβ plaques deposit. Rajendran et al. showed, about 20 years ago, that a fraction of Aβ can be secreted in association with EVs and that EV components co-deposit with Aβ in plaques [93] supporting physical interactions. Other studies have further associated both APP [143, 144] and Aβ [134] to EVs, and a role of EVs in prion-like propagation of Aβ has been suggested [134]. Furthermore, disruptions in endolysosomal function, including dysregulation of lysosomal acidification [145, 146] and endosome enlargements [90, 147] have been reported in relation to AD and Aβ pathology. These alterations can affect Aβ accumulation and secretion as well as modulate EV release and the concentration of EV-associated Aβ [148].

EVs can also interact with Aβ in the interstitial space and could thus potentially affect Aβ extracellular self-assembly, yet our knowledge on this remains limited and few studies report on the EV role on Aβ aggregation. In **paper I**, I have shown that EVs have an inhibitory role on *in vitro* Aβ aggregation kinetics which seems independent of EV cell origin [43], where fibrils formed in presence of EVs are significantly shorter, suggesting that EVs could contribute to the formation of smaller, more toxic, Aβ species. This work is further discussed in chapter 6 (Original Work). At the start of the work conducted within this thesis, there were only a few studies that had suggested that EVs modulate Aβ self-assembly [102, 149] and none had investigated their role on Aβ aggregation kinetics. Additional studies that do not specifically investigate the EV role on aggregation kinetics of Aβ but that still provide evidence of extracellular Aβ-EV interactions show that EVs can bind to Aβ [150] and influence Aβ plaque deposition [151].

4.3.1 Lipids and Aβ

Brain lipid dyshomeostasis is common in AD [152]. The brain is highly enriched in lipids and Aβ is found in association with several lipid-rich cell structures including neuronal synapses [153] and mitochondria [154]. Furthermore, Aβ is trafficked through and accumulates in the lipid membrane rich endolysosomes, which have been found to be impaired in AD (see also Chapter 3.3). Processing of APP is believed to predominantly occur on membrane microdomains rich in cholesterol and sphingolipids and changes in levels of both these lipids leads to altered lipid raft organization, which in turn influences Aβ formation [155-157]. Gangliosides are also components of lipid rafts and specifically the GM1 ganglioside is abundant in neuronal membranes and found to interact with Aβ [158-160]. In **paper III**, an inhibitory role of GM1 containing lipid vesicles on Aβ self-assembly, by interference with primary nucleation, is reported [39].

How these AD-related lipid alterations translate to the EV lipidome is less well studied. This is, in part, because profiling of the EV lipidome has only recently gained attention [115]. What we do know is that the EV lipid membrane is enriched in cholesterol, sphingomyelin and

glycosphingolipids and contains lipid raft-like microdomains [115, 116]. This means that EVs can not only interact with Aβ through their joint pathway in endolysosomes but also that certain lipids, and lipid raft domains, can directly interact with and influence conformation, clustering, and self-assembly of Aβ. For example, Aβ-binding to EVs has been shown to occur through glycosphingolipid glycans on the EV surface [161]. More recent work in the EV lipid field has focused on using changes detected in lipid profiling of EVs from healthy and diseased states as potential biomarkers. Lipid profiling of AD postmortem human brain tissue has revealed that EVs are altered in PS, PE and PC lipid composition [162, 163], have a remodelled sphingolipid metabolism, increased free cholesterol and upregulated lipids specifically involved in the endolysosomal pathway [164], possibly reflecting impairments in this route.

5. Methodology

This chapter provides brief introductions to the key methods used throughout this thesis and outlines how each was applied in the presented work.

5.1 Aβ Recombinant Protein Expression and Purification

Recombinant Aβ(1-42) was used in all *in vitro* Aβ(1-42) experiments in **papers I-IV** and in some of the cell experiments in **paper IV**. The fluorescent Aβ(1-42) in **paper IV** was a synthetic variant with Hilyte488 labelled from Anaspec.

Aβ is a highly aggregation prone peptide and in aggregation experiments it is crucial to start from monomeric solution to accurately report on self-assembly kinetics. This requires high purity peptide solutions as starting material. Historically it has been common to use synthetically produced Aβ in aggregation kinetic studies. This, however, has several problems such as batch-to-batch variations causing irreproducibility, issues with appropriately dissolving the peptide into monomers, and relatively high costs. Using recombinant peptide has been useful in overcoming these drawbacks [165].

In my work, Aβ(1-42) was produced following a protocol established by Abelein et al. [166]. This protocol utilizes a modified N-terminal domain (NT*) of spider silk proteins (spidroins) as a solubility tag. This keeps the aggregation-prone Aβ(1-42) soluble at high concentrations during expression and purification and makes it possibly to produce and purify Aβ(1-42) in *E.coli* (here BL21(DE3)) at high efficiency. The NT*- Aβ(1-42) gene construct is depicted in Figure 8. Immobilized metal affinity chromatography (IMAC) was used to purify the NT*- Aβ(1-42) fusion protein, followed by cleavage of the fusion tag using tobacco etch virus (TEV) enzyme. IMAC, which utilizes immobilised metal ions, was used to bind the NT*-Aβ fusion protein via its Histidine tag, as histidine residues bind metal ions through their imidazole side-groups. Thereafter, size exclusion chromatography (SEC) was used to purify the Aβ(1-42) peptide. The purified peptide was then lyophilized and stored at -20 °C. SEC, also called gel filtration, uses a porous stationary phase that separates solutes by size; larger particles that cannot enter the pores elute more quickly whereas smaller particles enter the pores and therefore elute later.

To avoid problems with aggregation that often occur during dissolution and thawing of the Aβ(1-42) peptide, it was monomerized once more immediately prior to each aggregation kinetics experiment, by dissolution in 6 M guanidine hydrochloride and subsequent SEC. This resulted in Aβ(1-42) eluting as a single monomer peak.

Figure 8. Schematic of the NT*- Aβ fusion protein.

5.2 Aβ Aggregation Kinetics

The aggregation of monomeric Aβ(1-42) was monitored using Thioflavin T (ThT) fluorescence. ThT is a benzothiazole dye (Figure 9) whose fluorescence is low in solution due to intramolecular rotation around the central single carbon-carbon bond connecting the benzothiazole and

dimethylaminobenzene rings. However, upon binding to β-sheet-rich amyloid structures, this rotational freedom is restricted, resulting in a strong increase in fluorescence intensity and a shift in excitation maximum (from ~ 413 nm to ~ 440 nm). Due to this light-up property, ThT has become extensively used to monitor amyloid fibril aggregation [167]. ThT binding has been shown not to affect the aggregation kinetics of Aβ(1-42) at ThT concentrations below 20 μM [168]. In all work included in this thesis, a concentration of 5 μM of ThT was used.

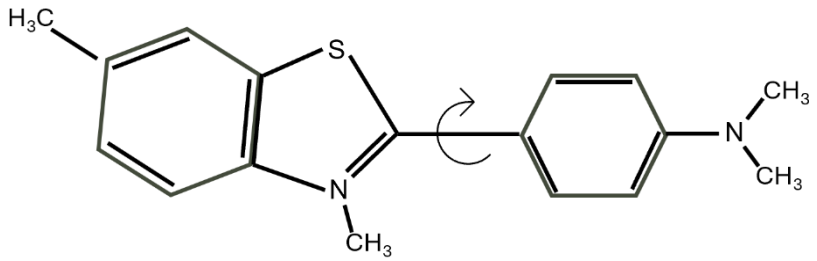

Figure 9. Structure of a Thioflavin T (ThT) molecule. The arrow marks the carbon-carbon bond around which the two rings can rotate.

There are other ways to measure amyloid aggregation kinetics besides using ThT fluorescence. These include other dyes such as Congo red which is used as a stain in amyloidosis diagnosis but is less suitable for *in vitro* experiments as it can interfere with amyloid formation of certain amyloid proteins [169], or more recently developed luminescent conjugated oligothiphene (LCO) type probes [170, 171].

5.2.1 Mechanistic models and analysis of Aβ aggregation kinetics

Monitoring aggregation kinetics is useful to explore and compare aggregation rates under different conditions and to analyse the effect of modifiers. However, to also understand the reasons why aggregation was changed, e.g. how a certain factor affects the underlying mechanisms of self-assembly, the aggregation curves must also be compared to mathematical models describing the aggregation process. In **papers I-III**, the kinetic traces were analysed using models available on the web-based platform Amylofit [11] to extract rate constants for the underlying aggregation steps (as explained in chapter 2.3).

Defining which of the microscopic steps in amyloid formation that are most prominently affected by a modulator is important for understanding its mode of action as well as to inform on possible downstream consequences in terms of amyloid fibril build-up and oligomer generation. Typically, multiple kinetic traces, spanning different protein or modulator concentrations, are analysed using global fitting to integrated rate laws, creating strong mechanistic constraints.

In my work, I fitted Aβ(1-42) kinetics using a multi-step secondary nucleation dominated aggregation model which describes the autocatalytic amplification of Aβ(1-42) fibrils via secondary nucleation [10, 11] and is further described in chapter 3.2. The term "multi-step" refers to secondary nucleation involving internal steps (such as (1) monomer binds to the fibril surface and then (2) converts into a new nucleus). This model therefore also accounts for the fact that secondary nucleation can saturate and lose its monomer-dependence at high monomer concentrations [172]. I used two fitting procedures, depending on whether the kinetics were

collected under unseeded or seeded experimental conditions. Under unseeded conditions, i.e. when the aggregation reaction starts from a purely monomeric solution, the model operates with the following parameters;

m_0 – initial monomer concentration

k_+k_n – combined rate constant of elongation and primary nucleation

n_c – reaction order of primary nucleation

k_+k_2 – combined rate constant of elongation and secondary nucleation

n_2 – reaction order of secondary nucleation

K_M – saturation constant

Because ThT fluorescence reports on total fibril mass, the observed kinetics depends on the overall rate of amyloid formation including both nucleation events and fibril elongation. Therefore, it is not possible to fit all individual rate constants to unseeded data. Instead, the kinetics are constrained by the products k_+k_n and k_+k_2. This means that fibril elongation cannot be separated from primary or secondary nucleation, but it is still possible to estimate which of the two nucleation processes that dominate. In **papers I-III**, I used the following approach to fit unseeded data; first, the model was fitted to aggregation of Aβ(1-42) in absence of any modulators to obtain initial estimates (initial guesses) of the fitting parameters. Next, the model was fitted twice to the aggregation kinetic data, allowing either k_+k_n or k_+k_2 to vary freely while keeping the other parameter constant. The purpose of this approach is to explore how well the changes in the kinetic curves induced by the modulator can be explained by variation in the free rate constant. Goodness of fit was used to determine the best fitting model and hence dominant mechanism.

In **paper I** and **III**, we acquired seeded kinetics, in addition to unseeded data, for a select number of conditions. Seeding predominantly eliminates primary nucleation but at high seed concentrations (25 %), elongation dominates over secondary nucleation, because the number of available free fibril ends become sufficiently high to allow monomers to be preferentially sequestered by elongation [173]. This makes it possible to separate k_+ from k_n and k_2 and hence understand the contributions from fibril elongation. Seeded experiments were performed by adding pre-formed Aβ(1-42) fibrils at a concentration of 5 or 25 %. The multi-step secondary nucleation dominated model was used also for seeded data, with the introduction of the following additional parameters:

P_0 – initial aggregate number

M_0 – initial aggregate concentration

These additional parameters describe fibrillar material present at the start of aggregation. M_0 was adapted to the seeding concentrations used in this thesis while P_0 was not independently specified (as it requires a knowledge of the seed length distribution).

5.3 Microscopy

5.3.1 Atomic force microscopy

Atomic force microscopy (AFM) was used in **papers I-III** to visualize individual Aβ(1-42) fibrils to inform about their morphology. AFM images were also analysed to determine lengths and heights of individual fibrils (**papers I-III**).

AFM is a type of high-resolution scanning probe microscopy in which a sharp tip, mounted on the non-reflective side of a flexible cantilever, scans a sample surface (Figure 10) to achieve topological or force information. As the tip interacts with the surface, attractive and repulsive tip-sample forces (such as van der Waals forces, electrostatic forces, dipole-dipole forces etc.) cause deflections of the cantilever. The cantilever motion is monitored by reflecting a laser beam, which is directed towards the reflective side of the cantilever, from the cantilever onto a photodiode that converts light into an electrical signal, enabling reconstruction of a high-resolution topographic map of the surface. Since the image in AFM is generated by the tip the resolution is thus not limited by light diffraction and AFM provides nanometre-scale resolution, well below the diffraction limit.

In this thesis, fibrils were imaged as dry deposits on mica. Mica is a crystalline material that, when cleaved, produces an atomically flat surface which is crucial for imaging objects on the scale of single nanometres. Since the freshly cleaved mica is hydrophilic and negatively charged, the mica surface was functionalized with (3-aminopropyl)triethoxysilane prior to adding Aβ(1-42) fibrils to introduce positive surface charge and improve fibril adsorption. Amyloid fibrils were visualized using semi-contact mode, in which the tip only intermittently contacts the surface. AFM image processing and quantitative analysis of fibril length and cross-sectional height were performed to assess if and how EVs affect the resulting Aβ(1-42) fibril morphology after aggregation.

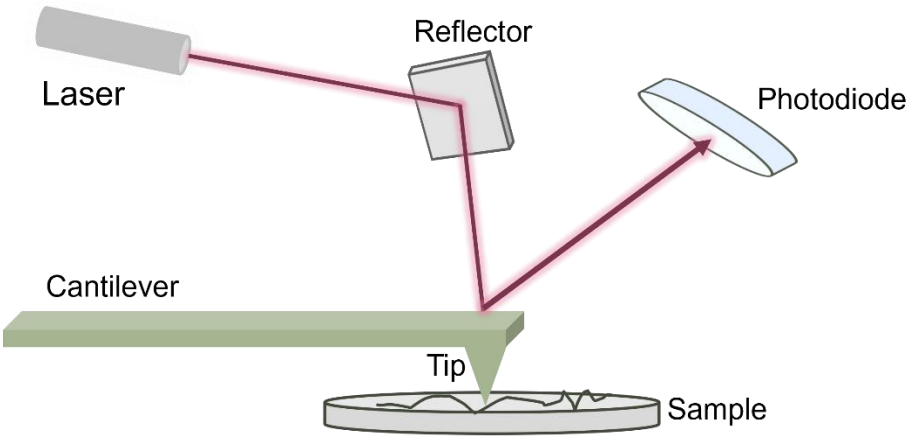

Figure 10. Schematic setup of an atomic force microscope.

5.3.2 Confocal microscopy

Confocal microscopy was used in **paper IV** to investigate the cellular uptake and accumulation of fluorescently labelled Aβ(1-42) peptides.

In fluorescence microscopy, light interacts with a specimen and is transmitted through an objective, resulting in a magnified image of the specimen. The Rayleigh criterion (Equation 2) explains the resolution (*d*) of the microscope, defined as the smallest distance between two sample points that can still be distinguished as separate objects. The resolution is determined by the wavelength (λ)of the incoming light and the numerical aperture (*NA*) of the objective.

$$d = 0.61\frac{\lambda}{NA} \qquad (2)$$

The *NA* of a microscope objective describes the objective's ability to gather light and is determined by the refractive index of the immersion medium between the objective and the object of interest and the angular aperture (half the angle of the of the cone of light that the objective can collect) of the lens. A higher *NA* increases the resolution of an image.

Confocal laser scanning microscopy (CLSM) and spinning disk confocal microscopy (SDM) were used in this thesis. In a confocal microscope (Figure 11), the specimen is excited by a focused laser beam that is reflected towards the objective and the specimen by a dichroic mirror. The emitted light passes through the objective and the dichroic mirror which separates it from the excitation light, allowing it to reach the pinhole placed in front of the detector. This pinhole allows for imaging of the focal plane, i.e. exclusion of out-of-focus light in both xy and z directions, thereby increasing the resolution of images acquired of thicker samples such as mammalian cells compared to standard fluorescence microscopy. In CLSM, the excitation laser is scanned across the specimen to construct the image. SDM builds on the same principle as CLSM but can achieve much faster image acquisition using a rapidly rotating disk containing thousands of small pinholes which allows for simultaneous scanning of multiple points of the specimen, as the emitted light is projected onto a camera.

Fluorophores can be attached to different biomolecules through various approaches. In this thesis, I have mainly used fluorescently labelled EVs that genetically encode mCherry as a fusion tag to an EV marker, in this case the tetraspanin CD63, and Aβ(1-42) fluorescently labelled with HiLyte Fluor 488.

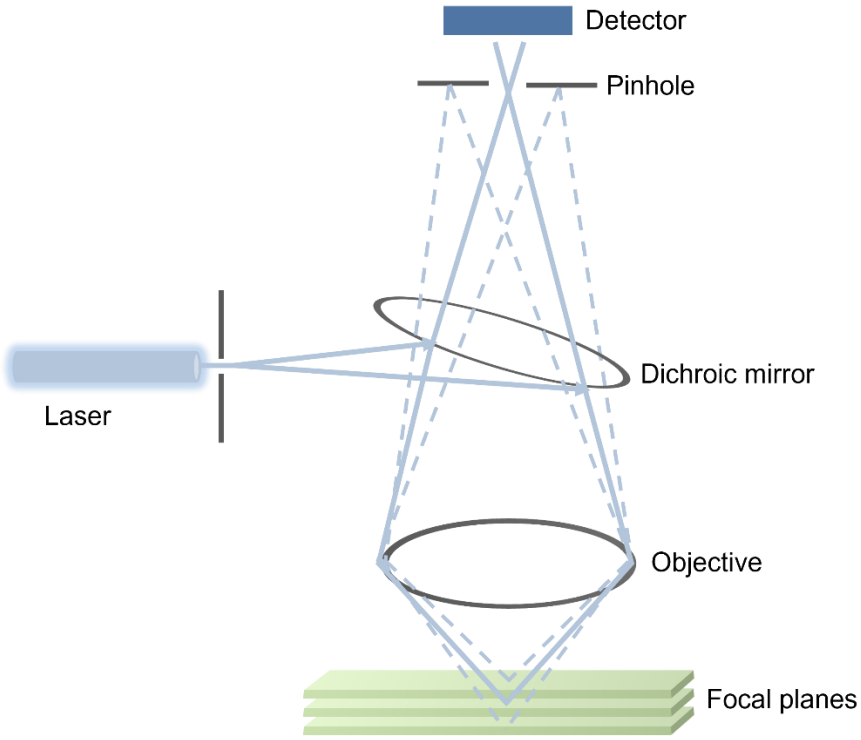

Figure 11. Schematic setup of a confocal laser scanning microscope.

5.4 Flow Cytometry

Flow cytometry was used to quantify the cellular uptake of fluorescently labelled Aβ(1-42) and EVs (**paper IV**).

Flow cytometry is a technique that measures physical and chemical characteristics of cells or particles. In flow cytometry, cells suspended in a fluid are injected into a detection chamber such that individual cells pass through a laser beam, as seen in the schematic (Figure 12). The flow cytometer used in this thesis utilizes a conventional hydrodynamic focusing where the sample is subjected to a sheath fluid with a laminar flow, confining the sample stream and ensuring that cells pass one-by-one. As the stream of cells passes one or several laser beams, the cells will scatter light, and any fluorescent markers matching the laser wavelength will be excited and emit light. Detectors then measure the emission as well as the scattered light, the latter both in the forward side scatter (FSC) direction, which scales with particle size, and in the side scatter (SSC) direction, which reflects internal complexity/granularity. The so-called FSC/SSC dot plot, where analysed cells are depicted based on their scatter, is an important feature in flow cytometry as it allows different cell populations to be distinguished. Dead cells, debris, or cell clumps scatter differently from live monodispersed cells, making it possible to gate the collected data such that the viable monodispersed cell population is included in downstream analysis.

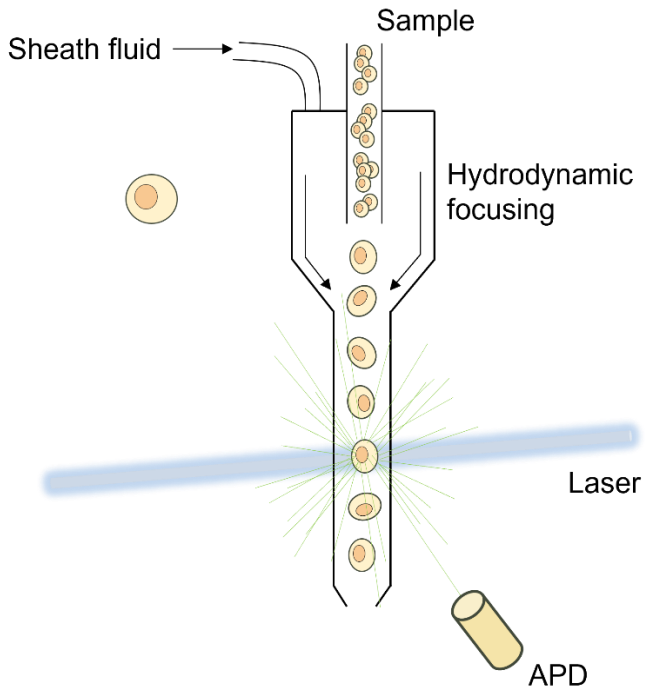

Figure 12. Schematic of a flow cytometer with conventional hydrodynamic focusing and avalanche photodetectors (APDs).

5.5 EV Isolation and Characterization

EVs are released by essentially all cell types and can be isolated from a wide range of biological media including cell culture medium, tissues, and all major biofluids (plasma, cerebrospinal fluid, urine, saliva, breast milk and others). There can be a significant overlap in size between EVs and other non-EV particles such as protein aggregates and lipoproteins which can be present in samples to various extents. Because of this, EV isolation is often considered as an enrichment process rather than a complete purification. Common EV isolation techniques include ultracentrifugation (differential or density gradient), SEC, ultrafiltration (UF), tangential flow filtration (TFF), and immunoaffinity capture. When choosing a method for EV isolation several aspects should be considered, including the starting material from which the EVs will be isolated, its major contaminants, the sample volume, and the balance between need for high purity and high yield. Another important aspect that should be considered is the downstream application, as not only EV purity but also integrity and function can be affected by the isolation procedure.

In this thesis, I have aimed for methods that enrich all EVs that are secreted in conditioned media of cultured cells. My studies are also constrained to EVs of a size below ~ 200 nm. Cells were cultured in serum free media to avoid protein contaminants and because the interstitial space surrounding neurons is serum free. Using serum free media furthermore removes the largest source of lipoprotein contaminants in cell culture derived EVs which are otherwise challenging to separate from the EVs since they overlap in size and density [174]. I used ultrafiltration as main method for EV isolation (**paper I-IV**), while tangential flow filtration was used to isolate some of the EV types used in **paper II.**

5.5.1 Ultrafiltration and tangential flow filtration

Ultrafiltration (UF) of EVs is conducted using membranes with molecular weight cut-off values that usually range from 10 – 300 kDa. In this thesis, UF was used to collect EVs from cell cultures in **papers I-IV**. Conditioned media (CM) from cells cultured in absence of serum was collected, centrifuged at low speed to remove cellular debris and larger particles, filtered and then ultrafiltrated twice at high speed, first to exchange culture medium to DPBS and second to concentrate the EV sample. UF is a fast, simple and relatively gentle method for isolating EVs.

Tangential flow filtration (TFF) is also extensively used for isolating EVs. In TFF, the CM is pumped parallel to the surface of a semipermeable membrane, usually of 100 – 300 kDa cut-off. Molecules smaller than the cut-off pass through the membrane as filtrate while larger particles, including EVs, remain in the retentate and are recirculated back to the sample reservoir. This method is useful for concentrating larger CM volumes without clogging the filter, which would be an issue when concentrating large volumes with UF. In **paper II**, some of the EV samples were obtained from collaborators that used TFF, in combination with UF, as EV isolation method.

5.5.2 Nanoparticle tracking analysis

NTA is a technique that is widely used to determine the size distribution and concentration of nanoparticle samples (20 – 1000 nm size range) [175]. In NTA, particles suspended in liquid are illuminated by a laser beam, causing them to scatter light and become visible under an optical microscope and possible to detect by a camera which is used to record short videos of the particles within a set field of view. The videos are than analysed by the instrument software to obtain each particle's trajectory, from which its Brownian motion and hence diffusion coefficient can be determined. The measured diffusion coefficient is used to calculate the particle's hydrodynamic diameter via the Stokes-Einstein equation (Equation 3) and under the assumption that particles are spherical.

$$D = \frac{k_B T}{6\pi\eta r} \tag{3}$$

Where:

D = translational diffusion coefficient

k_B = Boltzmann constant (1.380649 x 10^{-23} J/K)

T = absolute temperature

η = dynamic viscosity of the fluid

r = hydrodynamic radius of the particle

NTA is commonly used in EV research because it provides a rapid and non-destructive readout of size distribution and particle concentration [104]. Determining the EV concentration by NTA allowed for normalization of EV samples to the same starting concentration prior to aggregation kinetics and cellular uptake experiments. It also allowed to determine any size- differences between different EV samples, which became especially important in the setup of methods to determine the effect of trypsin-mediated removal of EV surface proteins in **paper II**.

6. Original Work

This chapter describes the main findings in this thesis (**papers I-IV**). First, the role of different cell-derived EV types on Aβ aggregation kinetics is presented (**papers I-II**). This is followed by a summary on how EV surface components such as proteins and proteoglycans, together with lipids commonly found on EVs and cellular membranes, each play a role in Aβ aggregation (**papers II-III**). Finally, the bidirectional crosstalk between EV and Aβ is discussed, highlighting how EVs modulate Aβ cellular uptake and how endolysosomal accumulation of Aβ peptides, in turn, alters EV release and composition (**paper IV**).

6.1 Extracellular vesicles slow down Aβ fibril formation and alter Aβ fibril morphology

EVs have been extensively explored across many subdisciplines of biology and medicine for their diverse roles in both physiological and pathological cellular states [95, 176]. They have been implicated as biomarker candidates and well as future therapeutic tools [103] across a wide range of diseases, including AD. However, the exact role of EVs in AD remains unclear. When I started my PhD, there were some reports suggesting that EVs could function as carriers in prion-like Aβ cell-cell transfer and influence various aspects of Aβ but there were no biophysical studies that thoroughly investigated the ability of EVs to directly affect Aβ aggregation kinetics.

In **paper I**, I established EVs as inhibitors of Aβ aggregation by exploring how EVs derived from human neuroblastoma SH-SY5Y and embryonic kidney HEK293-T cell cultures modulate the kinetics and mechanisms of Aβ(1-42) aggregation. Using ThT-monitored kinetic assays, I found that both SH-SY5Y and HEK293-T derived EVs slowed down Aβ(1-42) aggregation (Figure 13a-c). A major finding in **paper I** was that the inhibitory effects of EV from two distinct cell sources were, in fact, highly similar. In **paper II**, I expanded this observation by showing that EVs from an additional four cell sources of different lineage have strikingly similar effects on Aβ(1-42) aggregation kinetics (Figure 14, Figure 19). This strongly suggests that the inhibitory effect that I had identified is not restricted to certain EV types, but rather a generic ability of EVs encoded by their surfaces.

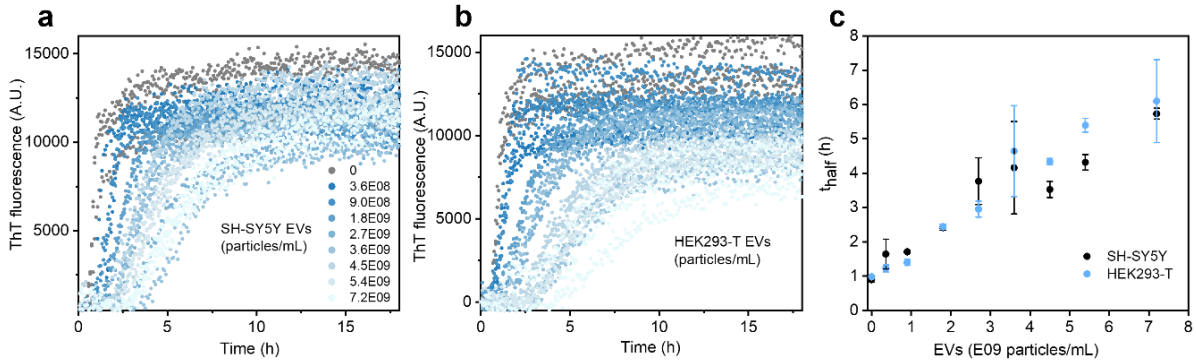

Figure 13. Aβ(1-42) aggregation kinetics in the presence of EVs. (a, b) Change in ThT fluorescence as a function of time, representing the aggregation kinetics of 2 μM Aβ(1-42) into amyloid fibrils in the presence of increasing concentrations of EVs isolated from (a) SH-SY5Y and (b) HEK293-T cells. (c) Reaction half-times extracted from the data in (a, b). The error bars represent the standard deviation (n = 3).

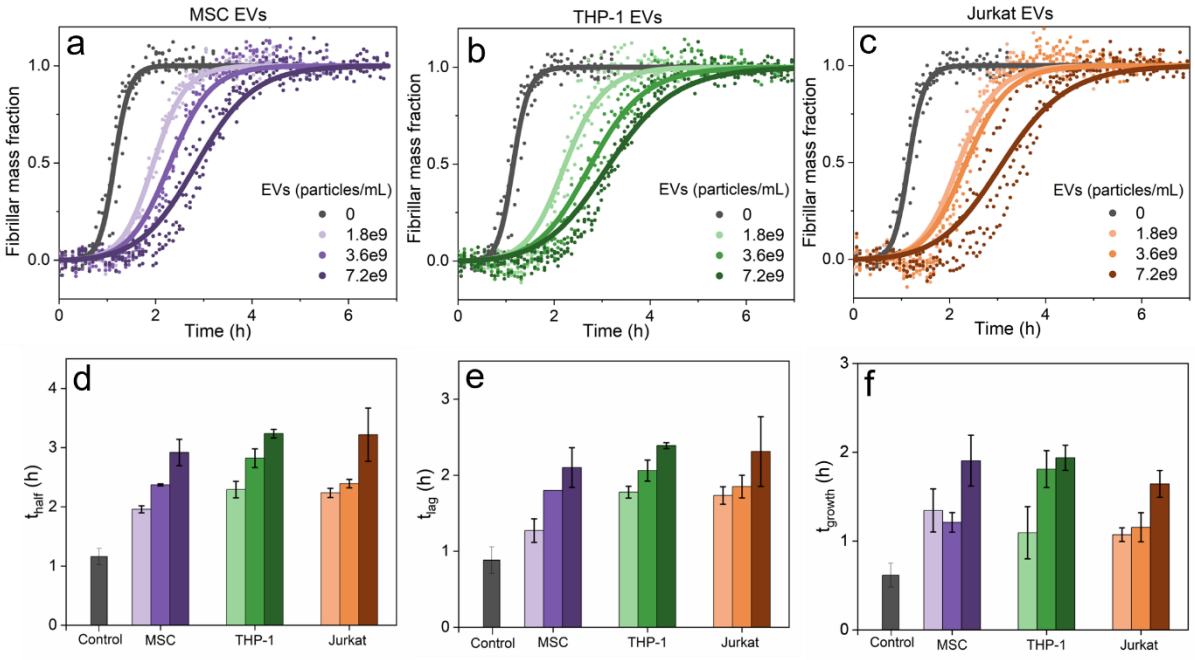

Figure 14. Aβ(1-42) aggregation kinetics in the presence of cord-blood derived MSC, THP-1 and Jurkat EVs. (a-c) Normalized ThT fluorescence assay over time showing Aβ(1-42) aggregation (2 μM) in absence or presence of indicated EV concentrations isolated from (a) umbilical cord-blood derived MSCs, (b) THP-1 cells, and (c) Jurkat cells. The dotted lines are experimental data points and the solid lines show fittings of the experimental data using a multistep secondary nucleation model of amyloid formation. (d-f) Reaction half-times (d), lag-times (e), and growth-times (f) extracted from (a-c). The error bars represent the standard deviation (n = 3).

In **paper I**, EV-mediated inhibition of Aβ(1-42) aggregation was observed at both low (5%) and high (25%) seed concentrations (Figure 15a-h). This is consistent with an inhibitory mechanism caused by EVs interfering with the fibril elongation step, which has been shown to dominate in reactions that proceed under high seed concentrations (high number of growth-competent ends) [173]. This interpretation was supported by mathematical fittings of kinetic models to the experimental data where the best fit was obtained when allowing the elongation rate constant (k_+) to vary freely whilst keeping the rate constants for primary nucleation (k_n) and secondary nucleation (k_2) fixed (Figure 15). In **paper II**, unseeded data were fitted to a model operating with two combined rate constants (k_+k_n and k_+k_2) where one was allowed to vary while the other was kept constant. This analysis identified that inhibition of secondary aggregation pathways (k_+k_2) is the dominant effect and thus excludes that EVs would modulate primary nucleation but could not directly discriminate between secondary nucleation and elongation. However, the observed changes to the kinetic curves, manifesting as prolonged lag and growth-times (Figure 14e-f) are consistent with the expected behaviour of elongation inhibitors [70].

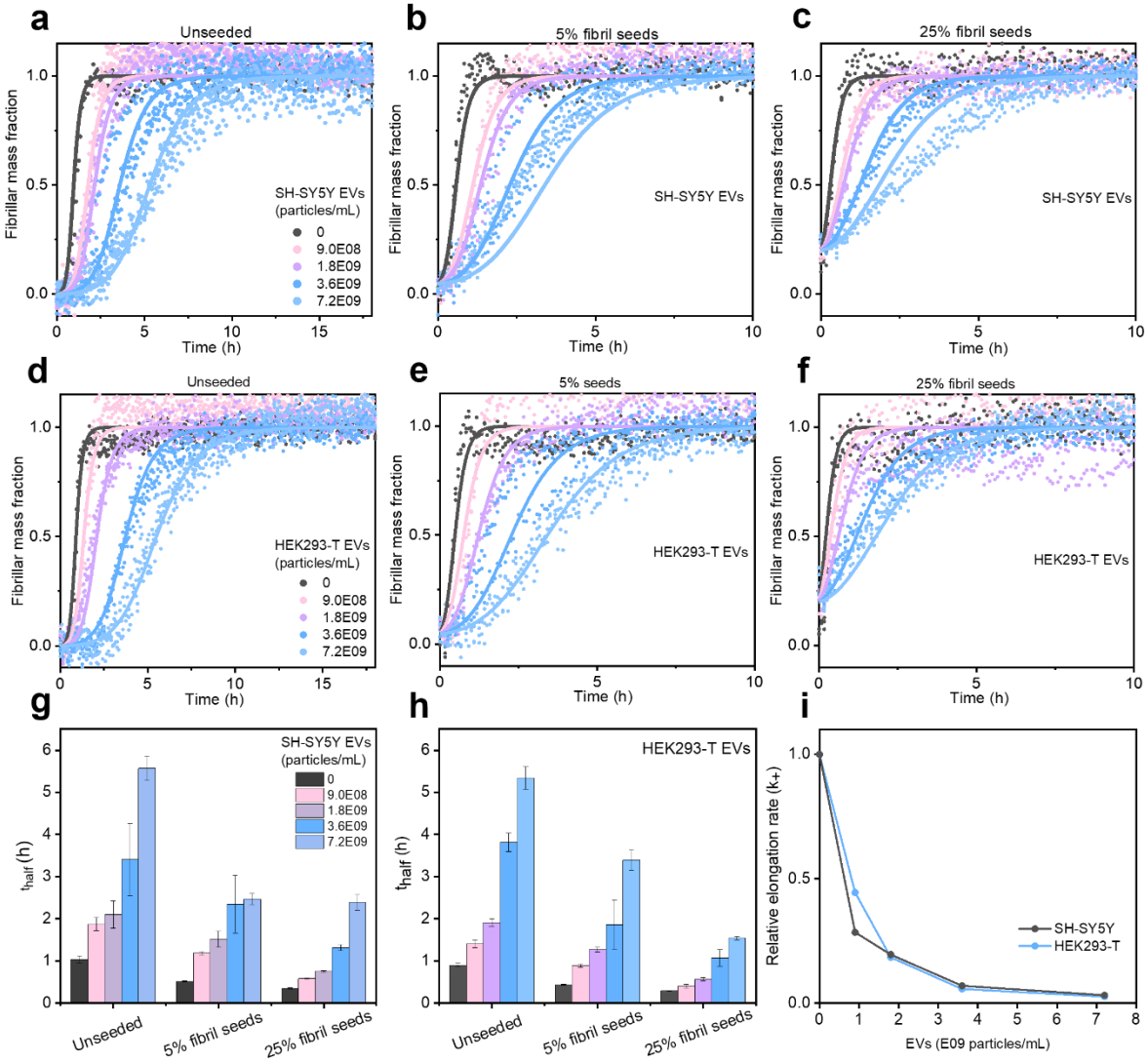

Figure 15. Effect of EVs on seeded aggregation of Aβ(1-42). (a-f) Normalized Aβ(1-42) aggregation kinetic curves showing the effects of EVs in absence (a, d) and presence (b, c and e, f) of 5 or 25 % preformed Aβ(1-42) fibril seeds. Panels (a-c) and (d-f) show data for SH-SY5Y and HEK293-T EVs, respectively. The solid lines were fitted using a multistep secondary nucleation dominated model of amyloid formation setting the rate constant for elongation (k_+) as a free parameter. (g, h) Reaction half-times as a function of EV and seed concentration, extracted from the data in (a-c, b-f). The error bars represent the standard deviation (n =3). (i) Change in the relative elongation rate constant (k_+) as a function of EV concentration, as determined by the fitting of the data in a-f.

Atomic force microscopy (AFM) was used in **papers I-II** to characterize the morphology of Aβ(1-42) fibrils, including determining their lengths and heights. The main finding from the AFM analyses was that all EV types reduced the length of Aβ(1-42) fibrils significantly (Figure 16a-d, Figure 17). In **paper I** we also performed cryo-TEM imaging of Aβ(1-42) fibrils which further confirmed the formation of shorter fibrils formed in presence of EVs (Figure 16f-k) and showed that these fibrils had altered morphology, including reduced apparent twisting of the fibril filaments (Figure 16h-k, vs f, g). The formation of shorter fibrils is consistent with elongation inhibition, as any inhibition of nucleation (primary or secondary) would rather reduce fibril numbers and hence favour the formation of longer fibrils.

Analysing fibril height could give insight into if EVs, or specific EV components, bind to and/or co-aggregate with the Aβ(1-42) fibrils, thus changing their thickness. In **paper I**, SH-SY5Y and HEK293-T EVs significantly increased Aβ(1-42) fibril height (Figure 16e), and cryo-TEM images showed small dark dots on the fibrils, as indicated by the white arrows in Figure 16i, suggesting possible co-aggregation of fibrils with EV material. However, such changes in fibril height were not observed with the EV types used in **paper II**. This suggests that if co-aggregation of fibrils with specific EVs or EV surface components occurs, it is likely a context-dependent process and involving the adsorption of proteins that are not directly responsible for the EV-mediated aggregation inhibitory mechanism. Taken together, these morphological analyses demonstrate that EVs not only delay Aβ(1-42) fibril formation but also confer distinct changes on the final morphological structure of Aβ(1-42) fibrils. Especially the formation of shorter fibrils is important as it strongly relates to a modulation of fibril elongation.

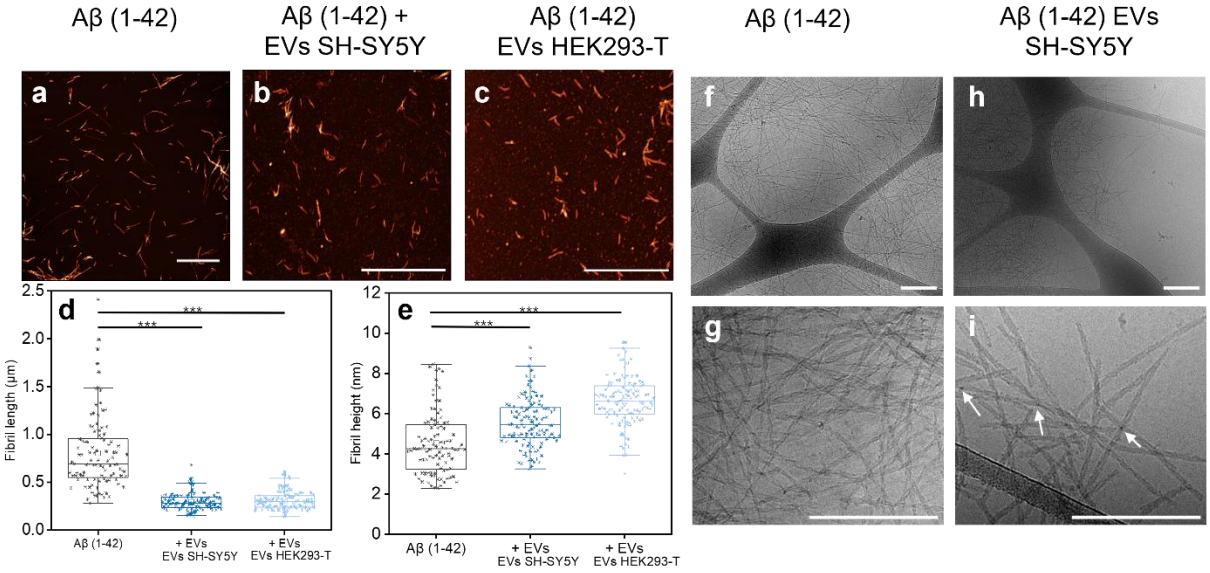

Figure 16. Morphological characterization of Aβ(1-42) fibrils formed in the absence and presence of EVs. (a-c) AFM images of Aβ(1−42) fibrils formed (a) in absence and (b, c) in the presence of SH-SY5Y and HEK293-T EVs. Scale bars = 2 µm. (d, e) AFM-based analysis of the distributions of (d) fibril lengths (e) and cross-sectional heights of the Aβ(1-42) fibrils formed in the absence and presence of EVs (n = 100−120 per condition, *** denotes $p < 0.001$ by one-way ANOVA). (f-k) Cryo-TEM images of Aβ(1-42) fibrils formed in the absence of EVs (f, g) or in the presence of EVs from, respectively, SH-SY5Y (h ,i) and HEK293-T (j, k) cells. The Aβ(1-42) fibrils formed in the presence of EVs contained small dark dots, indicated by the white arrows in (i) and (k), suggestive of the dense association of EV components. Scale bars = 250 nm.

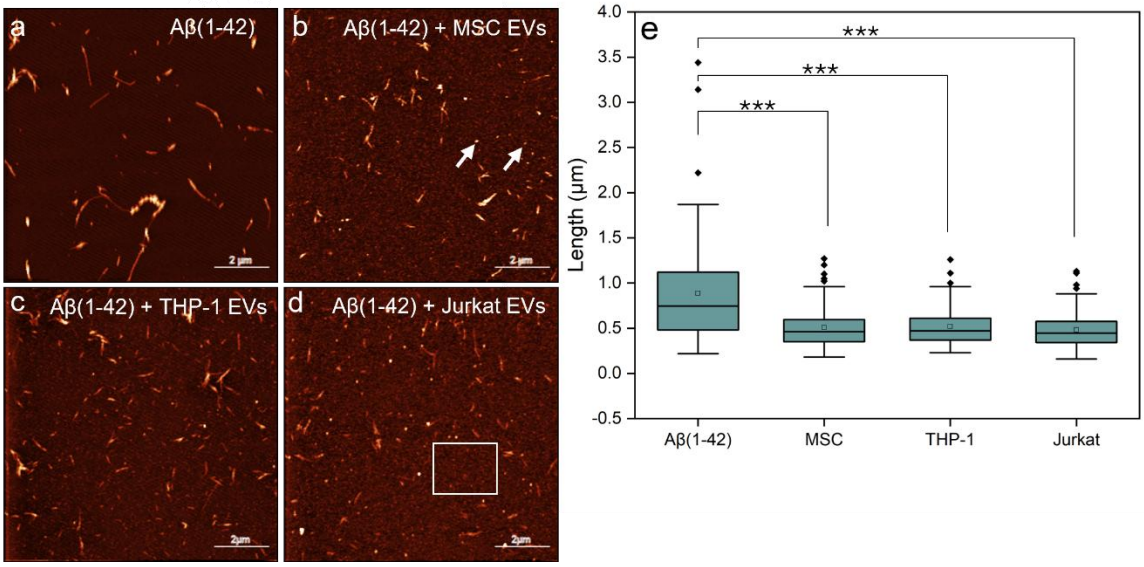

Figure 17. Morphological analysis of Aβ(1-42) fibrils formed in absence and presence of EVs. (a-d) Representative AFM images of Aβ(1-42) aggregation (2 µM) in absence (a) or presence of EVs from (b) umbilical cord-blood derived MSCs, (c) THP-1 cells, and (d) Jurkat cells. Scale bars = 2 µm. White arrows indicate smaller aggregate species in EV samples, and the white square marks the altered surface background in presence of EVs. (c) Analysis of fibril length based on AFM images of Aβ(1-42) fibrils (mean ± standard deviation, n = 100 fibrils from 11 images for the Aβ(1-42) + THP-1 EVs condition and from 10 images for the other conditions, *** denotes $p < 0.001$, by one-way ANOVA and Post-hoc Bonferroni-corrected means comparison tests) formed in absence and presence of the indicated EVs.

In summary, in **paper I,** I demonstrated that EVs slow down Aβ(1-42) aggregation kinetics and drive the formation of a fibril population with an overall significantly shorter length. I also showed that EVs can, thereby, act as regulators of extracellular Aβ(1-42) self-assembly by interfering specifically with fibril elongation. In addition, **papers I-II** collectively show that the aggregation modulatory effect of EVs is not confined to specific types but rather appears generic. I therefore proposed that aggregation inhibition is a common property of EVs that must be driven by a mechanism that is encoded in shared physicochemical or biochemical features of EVs and EV membranes, rather than by EV components that are specific to certain cell types. This conclusion could, at first, appear somewhat unexpected, as EV properties and characteristics have been shown to depend on cellular origin, and confer their functional specialization [114, 130]. However, this work does not necessarily contradict this idea but instead points out that EVs also share many physicochemical features. Indeed, EV commonalities are, for example, reflected in the difficulty of separating EV subtypes stemming from strong overlap in terms of both protein markers and size/density distributions. Delay in Aβ(1-42) fibril growth, as observed in **papers I-II**, could be interpreted as EVs being protective. However, the consistent observation throughout this thesis that EVs drive the formation of short fibrils, which are typically more soluble and generally associated with increased neurotoxicity [177-179], may also suggest that EVs interfere with Aβ(1-42) self-assembly in a way that enhances the accumulation of toxic Aβ(1-42) species, making interpretations about toxicity and overall consequences based on kinetic data less straightforward.

The major finding of **papers I-II**, namely that EVs have a common ability to slow down Aβ(1-42) aggregation kinetics and decrease fibril length, has formed the basis for the remainder of this thesis and motivated further work towards understanding how the EV surface confer its aggregation inhibitory effect.

6.2 The role of proteins, proteoglycans and lipids in EV - Aβ interactions

Following the finding that EVs slow down Aβ(1-42) aggregation kinetics I next wanted to further decipher EV components that contribute to this effect. In this, I focused on exploring the EV surface because this constitutes the interaction interface with Aβ(1-42) peptides. The EV surface, as described in chapter 4, can be considered as a complex lipid bilayer decorated with protein components and carbohydrates.

6.2.1 Surface proteins modulate the EV-mediated inhibition of Aβ(1-42) aggregation

The EV surface is highly enriched in proteins, both those that are firmly attached such as integral membrane proteins, and those that are more loosely associated (peripheral and corona proteins) [119, 180]. In recent years, the EV corona has increasingly been viewed not simply as a contaminant of EV preparations, but as an additional, functionally relevant, layer that can influence EV biodistribution, cellular interactions, and uptake [181, 182]. Here it is important to note that in my EV isolation setup, cells were cultured in serum-free medium; thus, any corona formed after EV release would be derived from cell-secreted biomolecules, not due to adsorption of serum proteins. All EV surface-associated proteins (integral, peripheral, and possible corona-proteins) could contribute to the inhibitory effect on Aβ(1–42) aggregation observed in **paper I**. This was further explored in **paper II** where EVs derived from human neuroblastoma (SH-SY5Y) cells were treated with trypsin, which cleaves peptide bonds at the carboxyl side of lysine and arginine residues, with the aim of proteolytically removing surface-exposed protein domains.

After the trypsin-treatment of EVs, I wanted to confirm successful removal of surface- associated proteins. However, there is a lack of methods to confirm the removal of said proteins, and the small amount of studies that have used trypsin to remove surface-associated proteins from the EV surface [183, 184] have done this either by showing a decrease in certain EV markers by western blot or by proteomics analysis. I sought to employ a method that does not quantify the reduction of specific proteins but rather conveys something about the total reduction of EV surface-associated proteins upon trypsin-treatment. I performed NTA analysis of untreated or trypsin-treated EVs, which showed a substantial decrease in mean EV diameter of ~ 8 nm (Figure 18a). The reduction in EV size corresponds to ~ 4 nm thinning of the EV particle radius. This decrease suggests a proteolytic trimming of surface-exposed protein domains and removal of surface-associated protein layers. The 8 nm decrease in diameter could suggest that SH-SY5Y EVs, as well as other EVs, contain a rather substantial EV corona. Next, I assessed surface protein removal by measuring intrinsic protein fluorescence from aromatic residues, tryptophan and tyrosine, in untreated and trypsin-treated EVs (Figure 18b). Trypsin-treatment resulted in a marked reduction in tryptophan fluorescence of ~ 80 %. This strong decrease in fluorescence further supports an extensive proteolysis of EV surface proteins of both integral and peripheral nature. Importantly, analysis of the flow-through of the ultrafiltrated untreated EV sample showed negligible tryptophan fluorescence of untreated EVs, whereas the flow-through from trypsin-treated EVs displayed increased fluorescence accompanied by a red-shift in emission (Figure 18c). This spectral shift is consistent with tryptophan residues becoming more solvent-exposed, as expected for at least partially unfolded peptide fragments [185].

After confirming that trypsin treatment resulted in significant removal of EV surface-associated proteins, I next assessed their effect on Aβ(1-42) aggregation kinetics. The trypsin-treated EVs not only retained the ability to delay Aβ(1-42) aggregation but the magnitude of inhibition was also

substantially increased (Figure 18d-e). Collectively, these data demonstrate that surface-accessible EV proteins contribute to the EV-mediated modulation of Aβ(1-42) aggregation and that proteolytic removal of them substantially enhances inhibition. It is possible EV surface proteins restrict Aβ(1-42) interactions with the EV membrane lipids and that by removing these proteins Aβ(1-42) species can more readily interact with the lipid bilayer. The role of EV lipids on Aβ(1-42) aggregation is further explored in **paper III**.

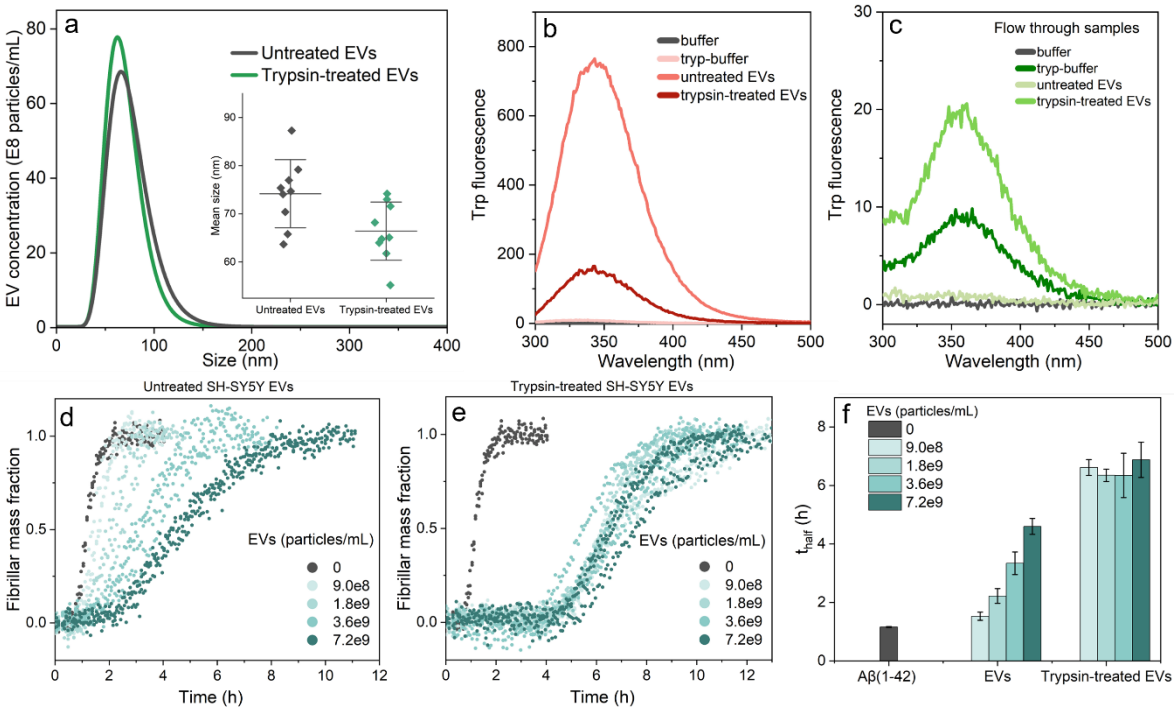

Figure 18. Characterisation of EV surface protein digestion after trypsin-treatment and their effect on Aβ(1-42) aggregation kinetics. (a) Size distributions and concentrations of SH-SY5Y EVs, untreated (black) or trypsin-treated (green) as determined by NTA. (b-c) Tryptophan (and tyrosine) fluorescence of EV samples (b) and flow-through (c) after trypsin-treatment and removal of peptide fragments and trypsin after ultrafiltration. (d-e) Normalized aggregation kinetics of 2 μM Aβ(1-42) in absence or presence of untreated (a) vs trypsin-treated (b) SH-SY5Y EVs on Aβ(1-42) aggregation kinetics. (c) Reaction half-times as a function of EV concentration, derived from the data in a-b.

6.2.2 EV-associated proteoglycans have minor impact on Aβ(1-42) aggregation

I also investigated whether EV-associated proteoglycans with their GAG chains contribute to modulate Aβ(1-42) aggregation. Proteoglycans are important for EV cell interactions and uptake [109, 128]. Furthermore, heparan sulfate proteoglycans (HSPGs) co-deposit with Aβ in plaques [186] and can promote cellular accumulation of Aβ and regulate Aβ toxicity [187-189].

I first compared untreated to heparinase II-treated SH-SY5Y EVs with respect to their ability to slow down Aβ(1-42) aggregation. Heparinase II removes specifically the HS GAG chains, such as syndecans and glypicans, leaving other non-HS GAGs (e.g. chondroitin sulfate) largely unaffected. Figure 19a shows that both untreated and Heparinase II-treated EVs slow down aggregation kinetics of Aβ(1-42), with a slightly stronger inhibitory effect of Heparinase II-treated EVs, as seen in the increased aggregation half-times. In parallel, EVs from CHO hamster ovary cells with normal (K1) and deficient (pgsA-745) GAG expression were compared. The latter are

xylotransferase I deficient and completely lack GAG chains [190]. A similar trend was observed, where EVs from both cell lines slowed down Aβ(1-42) aggregation kinetics, but GAG-deficient EVs possibly producing slightly stronger inhibition (half-times in Figure 19b). Importantly, the effect of enzymatically or genetically removing protein-associated GAGs was less pronounced than that observed upon removal of EV surface proteins, suggesting that they are minor contributors to EV-mediated modulation of Aβ(1-42) aggregation.

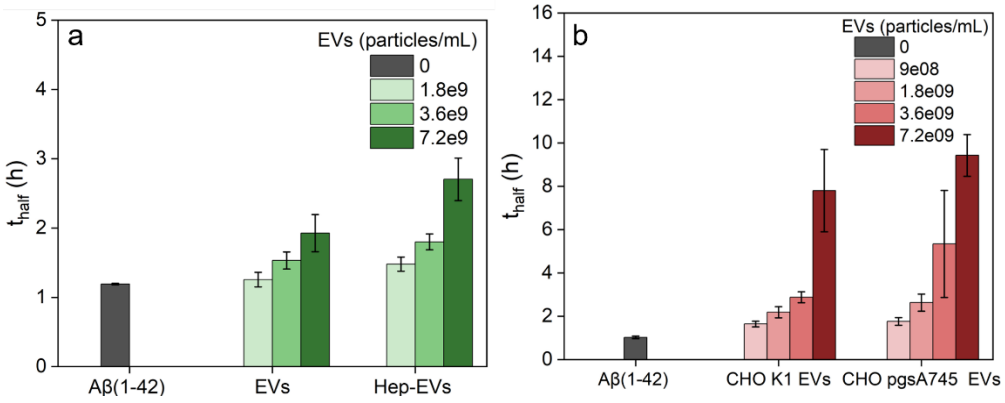

Figure 19. The effect of EV proteoglycans on Aβ(1-42) aggregation kinetics by glycosaminoglycan modified vs non-modified SH-SY5Y and CHO EVs. (a-b) Half-times extracted from Aβ(1-42) aggregation kinetics in presence of (a) SH-SY5Y EVs, untreated or Heparinase-II treated, and (b) Aβ(1-42) aggregation kinetics in presence of EVs from wildtype CHO-K1 cells or pgsA-745 mutant CHO cells.

In conclusion, the work in **paper II** contributes to better understanding of the origin of the generic inhibitory role of EVs on Aβ(1-42) fibril formation by identifying EV surface proteins as a significant regulator, whereas protein-attached carbohydrates on the EV surface appear to have comparatively minor effects. Interestingly, removal of both surface proteins and GAGs resulted in stronger aggregation inhibition. One interpretation of this finding is that the EV lipid membrane provides a particularly strong inhibitory interface for Aβ(1-42) aggregation, and that surface-associated proteins and carbohydrates somehow mask, or possibly even to some extent counteract, this effect. The role of lipids in Aβ(1-42) aggregation is the subject of **paper III.**

6.2.3 Lipids can delay and accelerate Aβ(1-42) aggregation

Several strategies can be used to investigate how the lipid portion of the EV membrane contributes to inhibit Aβ(1-42) fibril formation. In **paper II**, aspects of the lipid membrane's role were addressed indirectly by proteolytically removing surface proteins and enzymatically trimming GAG chains, thereby increasing the accessibility or exposure of the EV outer leaflet. The fact that the aggregation inhibitory effect of EVs was strengthened under these conditions points to the EV lipid membrane itself as an important regulator. In **paper III**, we instead used a bottom-up approach to examine how three AD- and EV-relevant lipids modulate Aβ(1-42) aggregation. A key aspect of **paper III** was to explore how the collective behaviours of lipids shape aggregation outcomes. This conceptually extended much of published work on lipid-mediated modulation of Aβ self-assembly, but is also especially important in the context of EVs, which have complex lipid

membranes and are known to contain both fluid and raft-like microdomains with putatively different effects and interaction potential with Aβ(1-42) peptides.

The basis of **paper III** was a panel of 20 different large unilamellar vesicles (LUVs) with systematic variation in lipid composition. They all contained DMPC as the base lipid, as this lipid does not affect Aβ(1-42) aggregation. They also contained different combinations (concentrations and ratios) of the AD pathogenesis-associated lipids ganglioside GM1, cholesterol (Chol) and sphingomyelin (SM) (Figure 20a). Sialylated gangliosides, such as GM1, have been reported to interact with Aβ peptides, often via clustering [158, 160], and to co-deposit with Aβ in plaques [191]. SM and Chol are, likewise, associated to AD pathology [77, 191, 192] and can, together with GM1, contribute to lipid raft formation which, in turn, facilitate GM1 clustering [193]. The lipids in **paper III** are also enriched in EV membranes [194] and have been implicated as important for EV membrane organization, EV secretion, and EV interactions with recipient cells [195].

Before proceeding to explore Aβ(1-42) aggregation kinetics, the membrane fluidity of a subset of the LUVs was assessed using laurdan fluorescence. This showed that the LUVs that contained mixtures of three or four of the assayed lipids, exhibited the highest membrane rigidity (Figure 20b), supporting the idea of lipid raft formation.

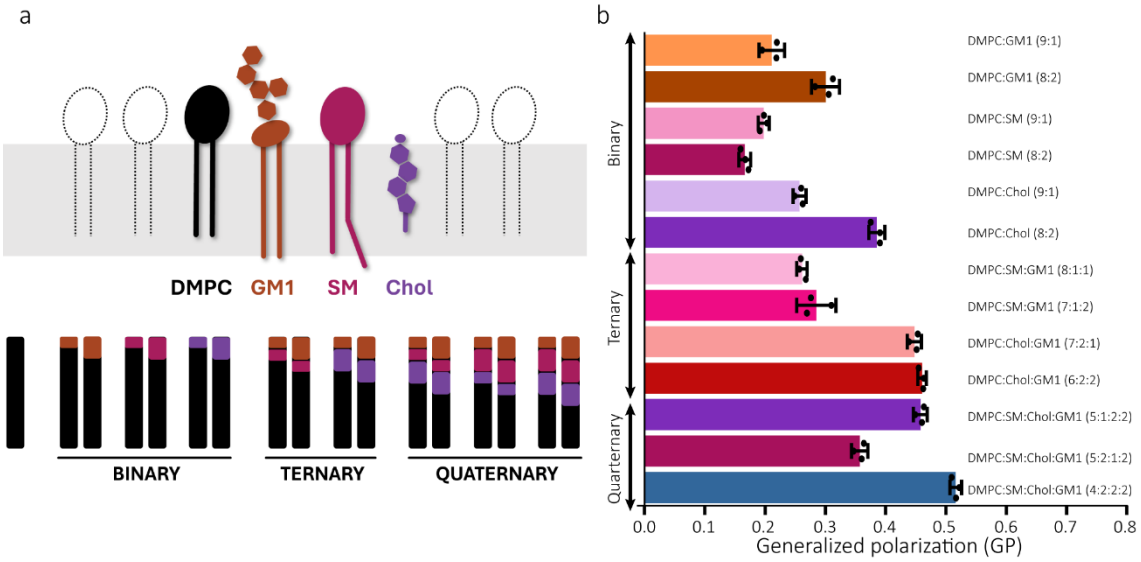

Figure 20. Structure and membrane fluidity of the lipid vesicles used in this study. (a) Schematic illustration of an idealised membrane with the lipids used in this study and a depiction of how they were mixed in different combinations to prepare large unilamellar vesicles (LUVs). (b) Laurdan fluorescence (generalized polarization, GP) of a subset of the LUVs to compare their membrane fluidities.

Thereafter the LUVs were used in aggregation kinetics experiments, exploring their effect on the fibril formation of Aβ(1-42). All kinetic data were analysed by fitting mathematical models of amyloid growth to understand how the different LUVs influence not only aggregation rates, but also the underlying microscopic Aβ(1-42) aggregation steps (Figure 21).

The results can be divided into three parts. First, we assessed the effect of the binary LUVs. This allowed us to determine the intrinsic aggregation-modulatory effects of the three key lipids (GM1, SM, Chol). We showed that GM1 slowed down Aβ(1-42) aggregation by interfering with the primary nucleation step, while SM and Chol both accelerated Aβ(1-42) aggregation, the first through interference with secondary nucleation and the latter through acceleration of primary nucleation, consistent with a published [196].

Next, we asked what would happen when lipids with opposing intrinsic effects on Aβ(1-42) aggregation were mixed into the same DMPC lipid bilayer. When these key lipids were mixed to form LUVs with three components (Figure 20a) we observed a competition between delay and catalysis (Figure 21c) between GM1 and Chol, where the Chol-mediated catalysis of Aβ(1-42) aggregation dominated at low total lipid concentrations and GM1-mediated delay dominated at high total lipid concentrations and high GM1 molar ratios. In LUVs with SM and GM1, the SM-associated catalytic effect on Aβ(1-42) aggregation was entirely dominant, overruling the GM1-mediated inhibitory effect. These findings contrast suggestions that individual lipids with opposing effects cancel out each other. Instead, one lipid effect can "win" and its effect can even be potentiated by the presence of a lipid with opposite intrinsic aggregation modulatory function.

Last, we explored the effects of lipid membranes with higher complexity by mixing all three lipids into DMPC bilayers. These high complexity LUVs had low membrane fluidity (Figure 20b), reflecting the ability of SM:Chol:GM1 mixtures to promote formation of lipid rafts. We observed overall strong inhibitory effects on Aβ(1-42) aggregation kinetics (Figure 21c) which resulted in reduced primary nucleation rates. These results show a second example of where, in this case, both Chol and SM seemingly give up their intrinsic catalytic behaviours and instead potentiate the inhibitory GM1-mediated effect on Aβ(1-42) aggregation kinetics. For example, Chol can increase spacing in the headgroup region of the bilayer, allowing Aβ(1–42) to engage in hydrophobic interactions at the surface and thereby exert a catalytic effect. However, in lipid rafts which are characterized by tight lipid packing this function of Chol is likely counteracted and instead Chol "gives up" its catalytic role in favour of promoting GM1-clustering.

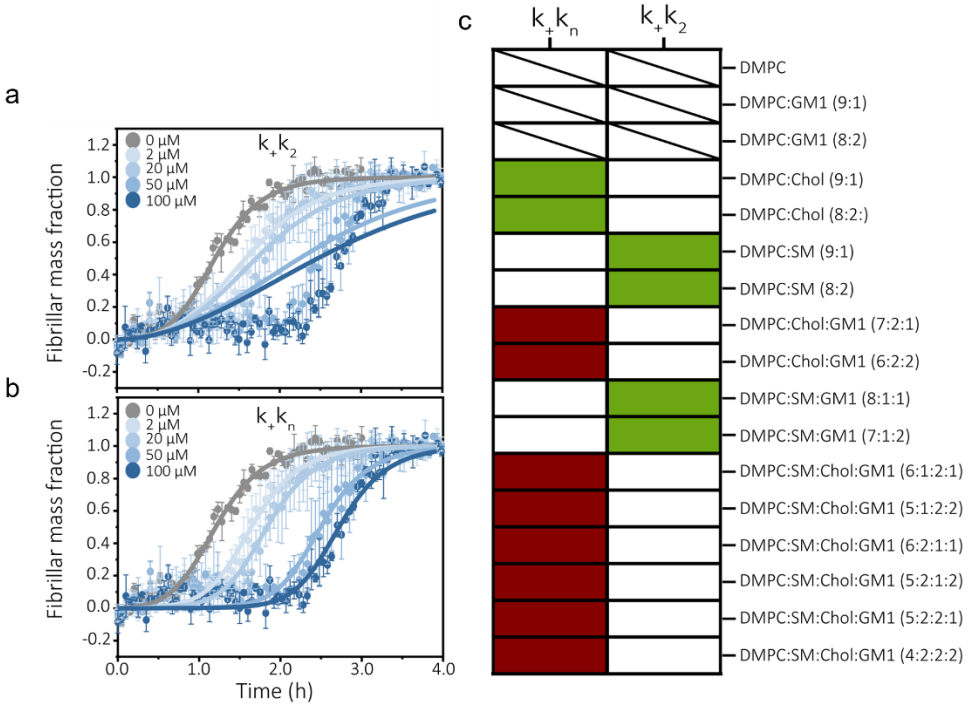

Figure 21. (a-b) Examples of the fitting of a secondary nucleation dominated kinetic model with saturation to experimental data of Aβ(1-42) aggregation in presence of DMPC:SM:Chol:GM1 (4:2:2:2) LUVs keeping either k_+k_2 (a) or k_+k_n (b) as the free parameter. Error bars represent standard deviation of three replicates. (c) Heat-map showing the best fitting kinetic model for each large unilamellar vesicle (LUV) type (e.g. if the change in aggregation rate is best described by variation in k_+k_n (left column) or k_+k_2 (right column)) determined based on smallest mean residual error (MRE). Green and red indicates catalysis and delay of aggregation (e.g. increase or decrease of the indicated rate constant) respectively. Dashed squares indicate that the data could not be fitted by the model.

In summary, this study expands our current understanding of how biological membranes modulate protein aggregation and addresses lipids that are relevant in the context of Aβ pathology. We show that the modulatory effect of lipid membranes on Aβ(1-42) aggregation is not only dependent on the chemical properties of individual lipids but also by their contribution to overall lipid membrane properties such as membrane fluidity. The modulation of Aβ(1-42) aggregation thus depends on the combined membrane properties that the lipids confer. Moreover, **paper III** is conceptually linked to my work on EVs in **papers I-II** and the suggestion in **paper II** that the lipid portion of the EV membrane is particularly aggregation inhibitory. Lipid rafts, which are enriched in cholesterol and sphingolipids, are important for EV formation [118] and have been studied in relation to EV biogenesis [197]. Consistent with this, EV membranes have been described as enriched in raft-associated lipids and to exhibit raft-like membrane organization. While this work cannot determine whether EV- mediated inhibition is specifically driven by GM1 clustering, the presence of such EV microdomains could create membrane environments that favour inhibition of Aβ(1–42) aggregation. This may help explain why EVs from different cellular sources exert similarly strong inhibitory effects on Aβ(1-42) aggregation.

6.3 EV-Aβ(1-42) crosstalk affects EV properties, Aβ(1-42) aggregation and accumulation

Research indicates that pathological cellular states can reshape EV composition [198] and, consequently, affect EV function [199, 200]. Such changes can include remodelling of the EV lipid membrane [201], for example altering organization of membrane microdomains [202], or alterations of the EV proteome by for example enriching proteins linked to stress and inflammation [203]. Because the EV surface is the first "contact point" with the extracellular environment it may also serve to alter EV interactions. This was the basis for the work conducted in **paper IV**.

Intracellular accumulation of Aβ is an early pathological hallmark of AD that appears concurrent with endolysosomal dysfunction including endosome enlargement and impaired lysosomal acidification [90-92]. In **paper IV**, I explored if Aβ(1-42) accumulation can modulate EV release. SH-SY5Y and HEK293-T cells were loaded with Aβ(1-42), resulting in endolysosomal accumulation, and then allowed to secrete EVs during a 24 hour period before collecting the EVs. EV secretion increased with this Aβ(1-42) pre-treatment (Figure 22 shows EV secretion from HEK293-T cells). One possible mechanistic explanation to this finding is if Aβ(1-42) accumulation impairs lysosomal degradation capacity and hence shifts cells toward alternative routes for handling and removing cargo, including secretion via EVs [94]. To assess this, uptake of pHrodo dextran 488, whose fluorescence increases upon delivery to acidic compartments, was followed in SH-SY5Y untreated or pre-treated with Aβ(1-42). Aβ(1–42) pre-treated cells showed a marked heterogeneity where a second subpopulation, approximately 20% of the total pHrodo Dextran positive cells, had a higher pHrodo Dextran signal (Figure 23a-c). These findings suggest that accumulation of Aβ(1–42) "overloads" the endolysosomal system, which could in turn alter EV secretion.

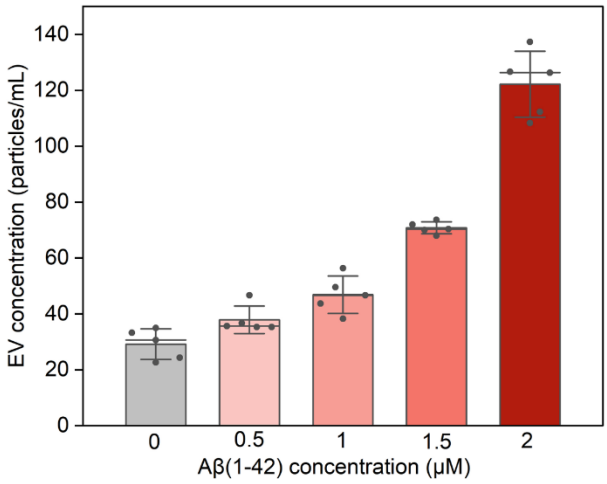

Figure 22. Aβ(1–42) exposure increases EV secretion. Quantification of CD63-mCherry HEK293T EV secretion from HEK293-T cells during 24h after a preceding 24h treatment of (1-42) with indicated protein concentrations. Quantification is based on mean ± standard deviation of five technical replicates (n = 5), determined with a micro/nanochannel device.

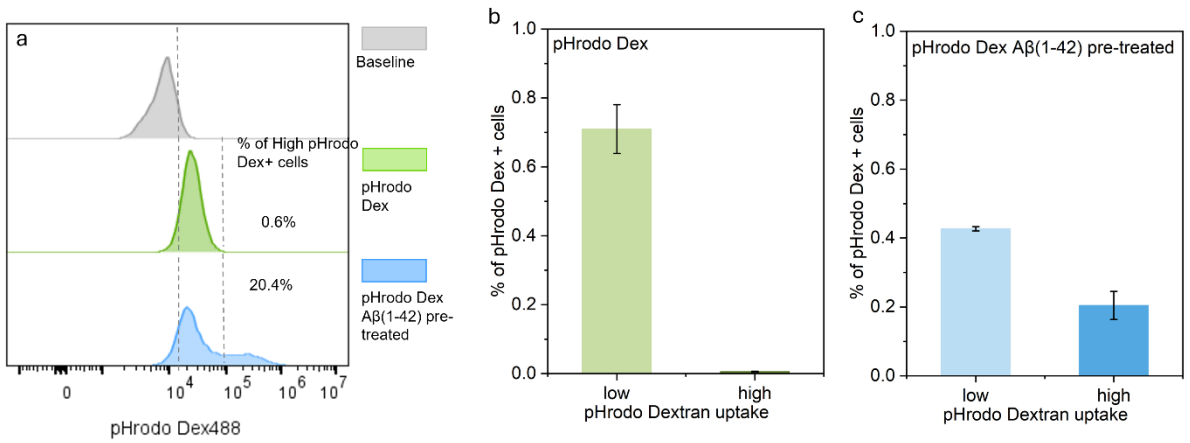

Figure 23. Aβ(1–42) cellular exposure alters endolysosomal acidification. (a) Flow cytometry histograms showing the cellular uptake of pHrodo dextran 488 at a concentration of 80 µg/mL after either untreated cells (green histogram) or a preceding 24h cellular treatment with 5 µM Aβ(1-42) peptide (blue histogram). The baseline representing cellular autofluorescence is shown in grey for comparison. The gating strategy defining the "high" pHrodo Dextran signal is shown with the percentage of pHrodo Dextran positive cells in untreated (green) and Aβ(1-42) pre-treated (blue) populations. (b-c) Quantification of the proportion of SH-SY5Y cells in the low and high pHrodo-Dextran signal gates for untreated (b) or (c) 5 µM Aβ(1-42) treated cells. Quantification is based on number of gated live single cells (10 000) and three biological replicates, with three technical replicates each (N, n = 3).

The next key question was whether EVs from Aβ(1-42) pre-treated cells are merely more abundant or also different in their interactions with Aβ(1-42). When comparing the effect of EVs from untreated vs Aβ(1-42) pre-treated cells, I found that EVs derived from Aβ(1-42) pre-treated cells exerted a stronger inhibitory effect on Aβ(1-42) aggregation kinetics (Figure 24a-c). Because EV function is tightly coupled to their composition, I performed quantitative proteomics to search for measurable changes that could potentially help define the altered aggregation modulatory effect. The data showed a clear separation between EVs from Aβ(1–42)-treated vs control cells in principal component analysis (PCA) (Figure 25a), indicating a treatment-associated change in EV protein composition.

Gene set enrichment analysis (GSEA) identified Reactome and Gene Ontology (GO) Biological Process gene sets with significant enrichment in EVs from Aβ(1-42) pre-treated cells, included pathways for membrane trafficking, Rho GTPase cycle, endosomal transport and vesicle organization (Figure 25b-d), supporting that Aβ(1-42) accumulation drives remodelling of the endomembrane system. Notably, the enriched set included AD-linked proteins such as membrane trafficking associated bridging integrator 1 (BIN1) and phosphatidylinositol binding clathrin assembly protein (PICALM) proteins which are both major risk factors for AD [204, 205] (Figure 26d). Enrichment of trafficking- and endosomal-related pathways could suggest increased activity in processes that regulate EV biogenesis, possibly providing a molecular context for the elevated EV secretion after Aβ(1-42) treatment. Proteins involved in glycosphingolipid metabolism were downregulated which could point to changes that result in altered membrane lipid composition that can influence EV surface properties and microdomain organization [162]. Such changes connect back to **paper III** and could lead to alterations in how EVs interact with Aβ(1-42), for example by altering binding capacity and strengthening their ability to modulate Aβ(1-42) aggregation.

The enhanced EV-effect that we note on Aβ(1-42) aggregation kinetics is likely related to changes that influence interactions of Aβ(1-42) and the EV surface. This could be inclusion/depletion of specific proteins or simply protein alterations that make the EV lipid membrane more accessible. Nevertheless, we therefore filtered our proteomic dataset for high-confidence surface-annotated EV proteins (n = 166) and examined their differential abundance (Figure 25e). This analysis revealed, for example, Aβ(1-42)-dependent remodelling of several chaperones, including HSPA5, and PDIA3/4. These EV-surface associated proteins [206, 207] are also linked to AD and Aβ pathology [208, 209] with proposed functions as aggregation inhibitors. However, these chaperones were down-regulated on EVs, which speaks against them having a direct role in EV-mediated Aβ(1-42). Instead, we speculate that their down-regulation in EVs is rather related to an increased cellular need of chaperones to respond to the endolysosomal Aβ(1-42) accumulation.

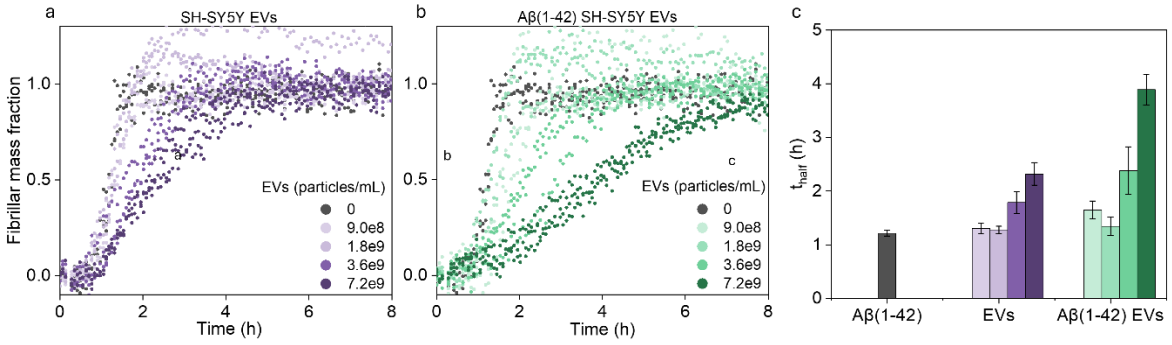

Figure 24. Aβ(1-42) aggregation kinetics in presence of SH-SY5Y EVs and EVs derived from Aβ(1-42) pre-treated cells. (a-b) Normalized ThT fluorescence assay over time showing Aβ(1-42) aggregation kinetics (2 μM) in absence or presence of (a) EVs from SH-SY5Y cells or (b) SH-SY5Y EVs from Aβ(1-42) pre-treated cells. (c) Reaction half-times derived from the aggregation kinetic curves in c-d. Colour scales represent the different EV concentrations used and indicated in c-d. The error bars represent the standard deviation (n = 3).

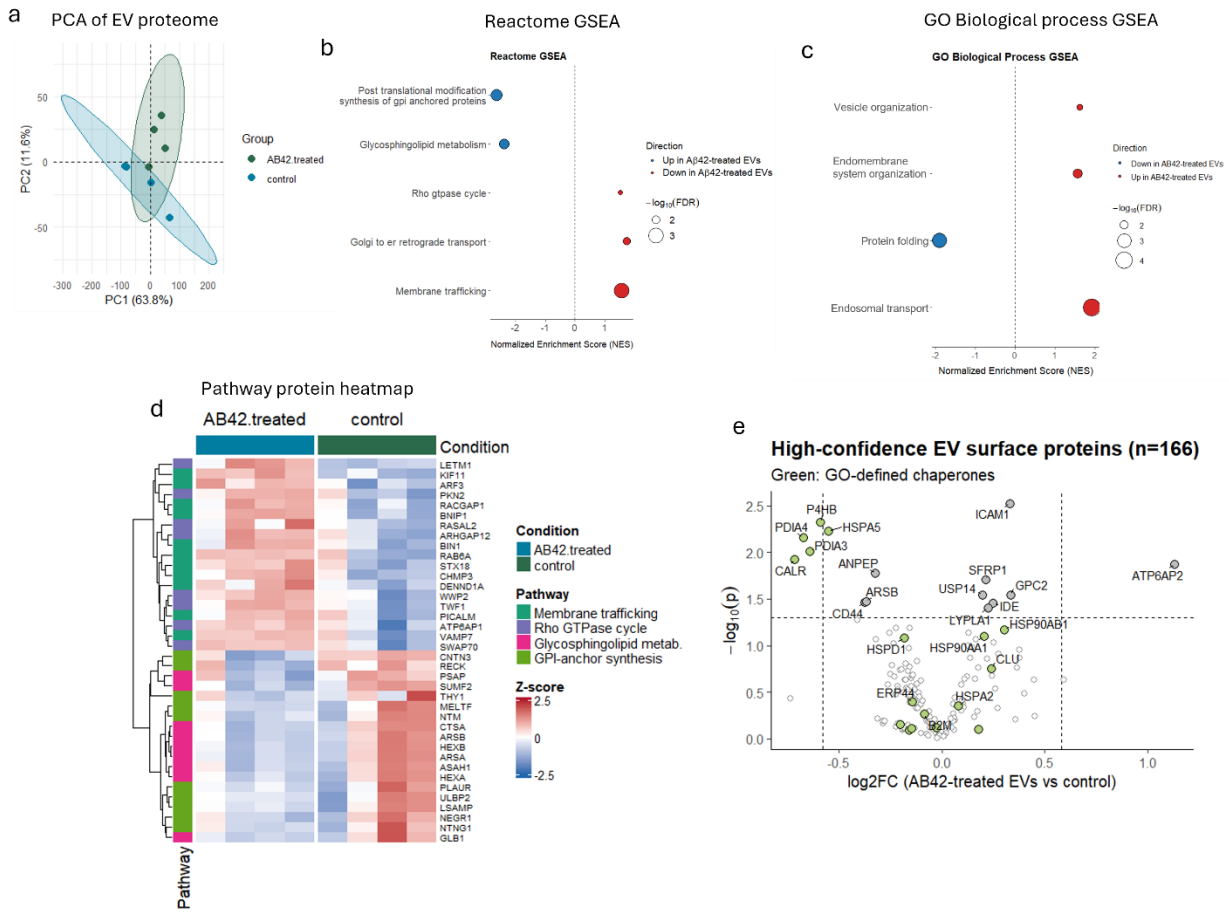

Figure 25. Aβ(1–42) exposure alters the EV proteome. EVs were isolated from SH-SY5Y cells left untreated (control) or pre-exposed to 1 μM Aβ(1–42) for 24 h (n = 4 per group) and analysed by quantitative proteomics. (a) Principal component analysis (PCA) of normalized protein abundances shows separation of EV samples by condition (originating from untreated or Aβ(1–42) pre-treated cells). (b) Reactome and (c) Gene Ontology (GO) Biological Process gene set enrichment analysis (GSEA) showing significantly altered pathways in EVs from Aβ(1-42) pre-treated vs untreated cells. Red indicates upregulation; blue indicates downregulation. Dot colour reflects normalized enrichment score (NES); dot size reflects false discovery rate (FDR), with larger dots indicating higher significance. (d) Heatmap of representative leading-edge proteins from significantly enriched Reactome pathways, showing scaled (row-wise z-scored) abundances across individual EV samples. Coloured sidebar indicates pathway membership for each protein (e) Volcano plot of differential protein abundance of high-confidence EV surface proteins (n = 166). (Aβ(1-42) pre-treated vs control) showing log2 fold-change versus –log10 adjusted p-value. GO-defined chaperones are coloured in green while other significantly enriched or downregulated proteins are coloured in grey.

Next, I investigated whether EVs themselves influence the cellular uptake and accumulation of Aβ(1-42). SH-SY5Y cells were co-incubated with HiLyte Fluor 488 (HF488)-labelled Aβ(1-42) and SY5Y EVs and the endolysosomal accumulation of Aβ(1-42) was quantified by confocal microscopy and flow cytometry. Co-incubation with EVs increased Aβ(1-42) uptake already after 4 h, as shown by representative confocal images and corresponding quantification (Figure 26a-c). Flow cytometry confirmed the EV-dependent increase and showed that it persisted over time. Furthermore, EVs from Aβ(1-42) pre-treated cells enhanced uptake even more than EVs from untreated cells (Figure 26d). To better understand why EVs would increase Aβ(1-42) uptake, I repeated the co-incubation experiments using mCherry-CD63 HEK293-T EVs. This EV type also increased Aβ(1-42) uptake (Figure 27a, c), showing that the EV uptake-promoting effect is not restricted to EVs of neuronal origin. The mCherry-CD63 EVs were also internalized, and both

EVs and Aβ(1-42) accumulated into distinct perinuclear puncta, consistent with trafficking into endocytic vesicles. Notably, the EV uptake was reduced when EVs were co-incubated with Aβ(1-42) compared to EV uptake alone (Figure 27d). In contrast, flow cytometry did not show a corresponding change in the total cell-associated EV uptake between EV only and Aβ(1-42) + EV conditions. These findings support a feed-forward loop where endolysosomal accumulation of Aβ(1–42) promotes EV release and remodels EV properties in such a way that that EVs in turn showcase stronger modulatory effect on Aβ(1–42) aggregation and enhancement of Aβ(1–42) intracellular accumulation.

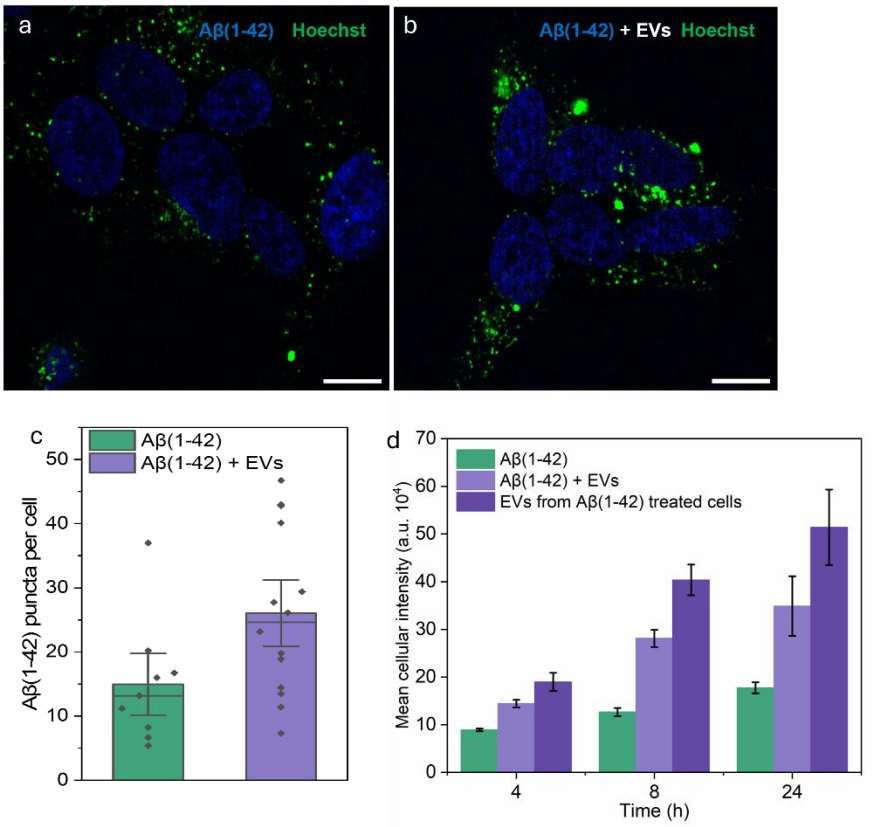

Figure 26. Imaging and quantification of the effect of SH-SY5Y EVs on Aβ(1-42) cellular uptake. (a-b) Representative confocal microscopy images of SH-SY5Y cells treated with 1 μM HF488-labelled Aβ(1-42) peptide after 4h incubation (a) without EVs or (b) with EVs. Scale bar = 10 μm. (c) Image-based quantification of the Aβ(1-42) cellular uptake. Each dot represents one analysed image; bars show mean ± SE (d) Quantification of Aβ(1-42) uptake in presence of EVs from untreated and Aβ(1-42) pre-treated cells by flow cytometry. The uptake is reported as mean cellular intensity ± SD of the total number of gated live single cells (10 000) for three replicates (n = 3).

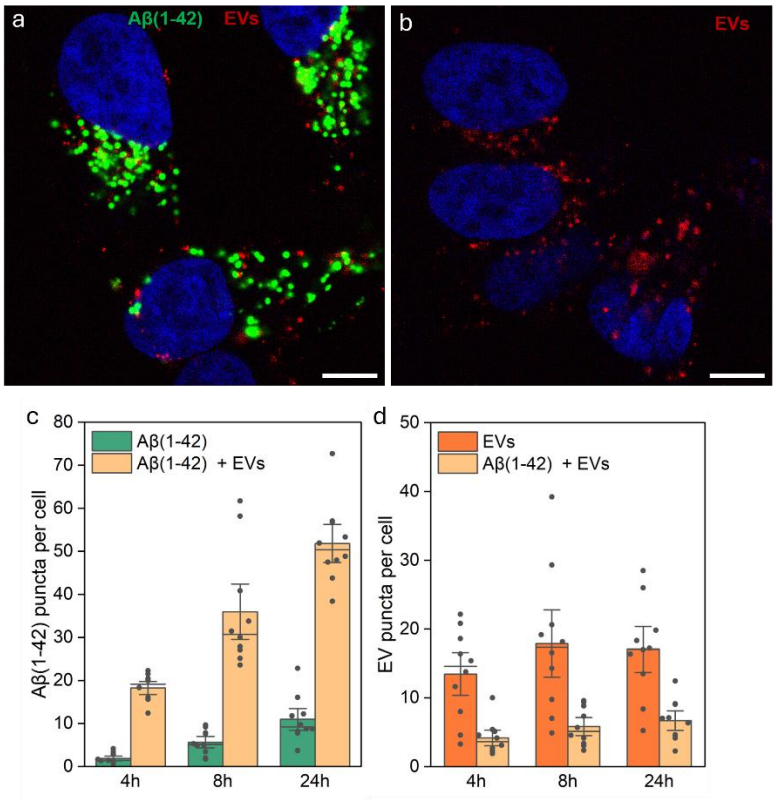

Figure 27. Imaging and quantification of Aβ(1-42) and CD63-mCherry HEK293T EVs cellular uptake. (a-b) Representative confocal images of SH-SY5Y cells incubated with (a) 1 μM HF488-labelled Aβ(1-42) monomers with CD63-mCherry labelled HEK293-T EVs or (b) CD63-mCherry EVs only for 24 h. Scale bar = 10 μm. (c) Quantification based on the confocal imaging of Aβ(1-42) puncta alone (green) or Aβ(1-42) and EVs (orange). (d) Quantification of EV puncta in cells treated with only EVs (orange) or EVs and Aβ(1-42) (light orange). Each dot represents one analysed image; bars show mean ± SE for c-d.

Paper IV expands on the bidirectional crosstalk between Aβ(1–42) and EVs and reports on a seemingly perpetuating loop where endolysosomal dysfunction caused by Aβ(1–42) accumulation can affect EV quantity and properties in such that EVs more strongly inhibit Aβ(1-42) aggregation while also conferring enhanced Aβ(1-42) accumulation. An interesting finding from this work was that EVs increased Aβ(1–42) accumulation and were themselves taken up, but with little to no co-localization with the internalized Aβ(1–42). This argues against a dominant "hitchhiking" mechanism where EV-bound Aβ(1–42) is co-internalized and instead suggests that EVs primarily act at the recipient cell surface (e.g. through receptor binding, membrane remodelling, or signalling) to facilitate Aβ(1–42) uptake. One possibility I initially considered was that EVs increase macropinocytosis, which is a possible internalization route of Aβ(1–42) [91]. However, EVs did not similarly increase dextran uptake, making a purely generic stimulation of fluid-phase endocytosis less likely and pointing instead to an effect that is at least partly specific to Aβ(1-42) and its uptake mechanism. I set out to explore this further in my work by inhibiting specific endocytic pathways with chemical inhibitors but was unable to set up an optimal assay within the timeframe of this thesis. Additionally, although we did not note a large effect of EV proteoglycans on Aβ(1–42) aggregation, one could perturb the EV glycocalyx which participates in EV interactions with recipient cells to test whether it contributes to the enhanced Aβ(1–42) uptake.

7. Concluding Remarks

Alzheimer's disease remains a major public health challenge and a leading cause of death worldwide. Over recent decades progress has been made in defining key molecular events in AD and the role of Aβ as a driver of AD pathology is well supported. Yet, we still do not have sufficient understanding of the factors that initiate Aβ aggregation and propagate accumulation. Recent advances with antibody-based therapies targeting Aβ load represent a promising step forward, but there is still a pressing need for disease-modifying treatments that can truly halt the progression of this devastating disease. This emphasizes the need for deeper knowledge of the cellular and molecular pathways that modulate Aβ production, clearance, trafficking, and accumulation. My thesis contributes to fill this knowledge gap by showing that extracellular vesicles (EVs) can act as active and direct modulators of both Aβ aggregation and accumulation. This work is important because it provides new insight into how Aβ pathology can proceed and be affected by components in the brain environment, which is, in turn, crucial for target identification as well as development of future effective treatments.

The core focus of my thesis has been to characterise the modulatory role of EVs on Aβ(1-42) aggregation. When I started my PhD, there were only a handful of published indications of that EVs could modulate Aβ self-assembly and neurotoxicity (see Chapter 4.3). My **paper I** was the first published biophysical study in this important area. In **paper I**, I demonstrated that EVs effectively slow down the aggregation kinetics of the disease-associated Aβ(1-42) variant and used kinetic modelling to show that EVs selectively interfere with the fibril elongation step. This is important because it directly identifies EVs as modulators of Aβ(1-42) self-assembly and shows that, while inhibitory, this elongation inhibition could prolong the lifetime of soluble fibril fragments which, in turn, could either be neurotoxic in themselves or act to sustain oligomer production through secondary nucleation and thus increase Aβ(1-42) toxicity. My findings thereby provide a possible explanation for why both promotive and deleterious actions of EVs have been reported in association with AD and Aβ pathology [93, 102, 149, 161] and supports the emerging view of EVs as context-dependent modulators. Another key finding of the work in **papers I-II** is that the inhibitory effect is not restricted to EVs from a single cell source but rather a generic and robust property that is independent of cell origin. This extends existing literature, which has largely emphasised cell-type-specific EV properties in the context of disease [101, 114, 210]. Finally, understanding which EV properties are responsible for this will not only be useful for understanding how these biological vesicles modulate disease mechanisms of Aβ pathology, but also for future use of engineered EVs or synthetic vesicle models as therapeutics.

Building on this, **papers II-III** addressed the next key question: which EV-associated components confer the modulation of Aβ(1–42) aggregation? First, in **paper II**, I set up a method for removing EV surface proteins and appropriately assess the effect by measuring changes in EV diameter and in tryptophan and tyrosine fluorescence. Using this approach, I could show that removal of surface-associated EV proteins strengthened the inhibition of Aβ(1–42) aggregation. This suggests that the EV surface proteome could partially mask or counteract a strong inhibitory interaction specifically related to the EV lipid membrane. The generic nature of the EV effect on Aβ(1–42) aggregation established in **papers I-II** makes it unlikely that inhibition is caused by specific protein(s) on the EV surface. Yet, understanding the EV surface proteome better is interesting because it can help us understand how these proteins contribute to modulate protein aggregation, probably by a combination of direct interactions and steric shielding of the lipid bilayer portion of the EV membrane.

I initially attempted to specifically map how trypsin-treatment altered the EV proteome using proteomics in combination with a commercial method for shaving off and collecting proteolytic fragments [211]. However, I experienced difficulties with attaining sufficient EV concentrations for proteomics and this part of my thesis work could not be completed. Instead, I used whole EV proteomic analysis in **paper IV**. Nevertheless, it would be interesting to continue to pursue proteomic analyses to learn which proteins that are removed by trypsin. It could thereafter, for example, be possible to construct simplistic EV-mimicking liposome models with selected protein components, to test their role in protein aggregation.

By removing surface-associated proteins, and also GAGs, (**paper II)**, I was able to show that the EV lipid membrane likely confers a strong inhibitory effect on Aβ(1–42) aggregation. The role of the lipid component was further explored in **paper III** using a different approach. Here we instead investigated the role of GM1, SM and Chol, three AD- and EV-relevant lipids, on Aβ(1–42) aggregation. When these three lipids were mixed into one membrane, they promoted the formation of low fluidity domains (e.g. rafts) which significantly enhanced GM1-associated Aβ(1–42) likely because lipid rafts facilitate GM1 clustering. This provides a conceptual bridge back to EVs, which are enriched in membrane microdomains and these specific lipids. Even though different EV populations may vary in overall lipid composition, certain lipid properties, including increased membrane rigidity and membrane microdomain formation are shared. This commonality may, in fact, be sustained across EVs of different lineages and could thus contribute to explain why all EVs inhibit Aβ(1-42) aggregation. Another contributor to lipid raft organization of biological membranes are proteins, which can partition to both high and low fluidity domains. Thus, it is possible that EV surface proteins indirectly participate to shape the EV modulatory effect on aggregation. Research on lipid raft-like domains on EVs is still relatively recent and often addresses the role of these microdomains in regulating EV biogenesis [197, 212]. An interesting next step from this work would be to further investigate lipid raft-like domains of EVs by for example creating more complex lipid bilayer systems with proteins incorporated and studying how these systems bind to and affect Aβ self-assembly.

Whereas **papers I-III** focused on the role of EVs in the context of Aβ(1–42) aggregation kinetics, the work presented in **paper IV** addressed both extracellular Aβ(1–42)-EVs interactions and how their intracellular pathways intersect. I showed that endolysosomal accumulation of Aβ(1–42) enhances EV secretion, and that these EVs in turn are more potent at inhibiting Aβ(1–42) aggregation and enhancing Aβ(1–42) accumulation, resulting in what seems like a perpetuating loop that could reinforce pathological trafficking of Aβ(1–42). The proteomics analysis, used descriptively in this work, demonstrated that Aβ(1–42) accumulation is associated with changes in the EV proteome, including both enrichment and depletion of AD and Aβ pathology-related proteins. This is in line with other work that have shown alterations of protein levels in EVs from CSF and tissue samples [213, 214] of AD patients. In addition, my work shows that EVs from Aβ(1-42) pre-treated cells are enriched in proteins related to membrane trafficking and vesicle formation, again emphasizing how these two entities affect each other. The results from the proteomics analysis could be used in future studies to investigate AD- and/or Aβ-related and EV-related proteins and their role on Aβ(1–42) accumulation and toxicity in more detail. The findings in **paper IV** suggest that while a shared membrane-driven mechanism may underlie the common inhibitory effect, the producing cell's pathological state can remodel EV composition and can result in an amplification of certain EV properties, including stronger aggregation inhibition and enhanced Aβ(1–42) uptake.

8. Acknowledgements

First, I would like to thank my supervisor, **Elin**, for your encouragement and support throughout these years, and for always believing in me. Your genuine passion and curiosity for research is a great inspiration, and talking to you about science is always uplifting and fun.

I would also like to thank my co-supervisor **Fredrik** and my previous and current examiners **Pernilla** and **Anna,** for your encouragement and interest in my work and for always being available when I needed your support.

To all friends and colleagues at the division. **Elin** and **Viktoria**, for your friendship and all the invaluable talks, both scientific and on other matters. **Loise**, **Eve**, **Hanna** and **Gizem**, for always being so uplifting and kind, and for all the good memories. **Fritjof**, for all the help in the lab, and for your optimism that everything will work out. **Nima**, for the fun collaborations, for being a great friend and for continuing to help me even after you left our group. **Karin, Marziyeh** and **Andrea**, for the support and the many fun discussions. **Ranjeet**, for always being so helpful and supportive, especially with the protein purification.

Last but not least, I want to thank my family. **Mamma**, **Pappa**, **Agnesa**, **Vjollca** and **Francesca**, your support and belief in me are unwavering and you are the best family I could hope for. **Ermir**, for your support and love, and for always making everything feel better.

9. References

1. W.H.O. *World Health Organization, Dementia*. 2025; Available from: https://www.who.int/news-room/fact-sheets/detail/dementia.
2. *Alzheimer's Disease International Dementia statistics*. 2025; Available from: https://www.alzint.org/about/dementia-facts-figures/dementia-statistics/.
3. Blennow, K., M.J. de Leon, and H. Zetterberg, *Alzheimer's disease.* Lancet, 2006. **368**(9533): p. 387-403.
4. Alzheimer, A., et al., *An English translation of Alzheimer's 1907 paper, "Uber eine eigenartige Erkankung der Hirnrinde".* Clin Anat, 1995. **8**(6): p. 429-31.
5. Glenner, G.G. and C.W. Wong, *Alzheimer's disease: initial report of the purification and characterization of a novel cerebrovascular amyloid protein.* Biochem Biophys Res Commun, 1984. **120**(3): p. 885-90.
6. Hardy, J.A. and G.A. Higgins, *Alzheimer's disease: the amyloid cascade hypothesis.* Science, 1992. **256**(5054): p. 184-5.
7. Kayed, R., et al., *Common structure of soluble amyloid oligomers implies common mechanism of pathogenesis.* Science, 2003. **300**(5618): p. 486-9.
8. Lue, L.F., et al., *Soluble amyloid beta peptide concentration as a predictor of synaptic change in Alzheimer's disease.* Am J Pathol, 1999. **155**(3): p. 853-62.
9. Walsh, D.M., et al., *Naturally secreted oligomers of amyloid beta protein potently inhibit hippocampal long-term potentiation in vivo.* Nature, 2002. **416**(6880): p. 535-9.
10. Cohen, S.I., et al., *Proliferation of amyloid-beta42 aggregates occurs through a secondary nucleation mechanism.* Proc Natl Acad Sci U S A, 2013. **110**(24): p. 9758-63.
11. Meisl, G., et al., *Molecular mechanisms of protein aggregation from global fitting of kinetic models.* Nat Protoc, 2016. **11**(2): p. 252-72.
12. Scheres, S.H.W., B. Ryskeldi-Falcon, and M. Goedert, *Molecular pathology of neurodegenerative diseases by cryo-EM of amyloids.* Nature, 2023. **621**(7980): p. 701-710.
13. Soderberg, L., et al., *Lecanemab, Aducanumab, and Gantenerumab - Binding Profiles to Different Forms of Amyloid-Beta Might Explain Efficacy and Side Effects in Clinical Trials for Alzheimer's Disease.* Neurotherapeutics, 2023. **20**(1): p. 195-206.
14. van Dyck, C.H., et al., *Lecanemab in Early Alzheimer's Disease.* N Engl J Med, 2023. **388**(1): p. 9-21.
15. Englund, H., et al., *Sensitive ELISA detection of amyloid-beta protofibrils in biological samples.* J Neurochem, 2007. **103**(1): p. 334-45.
16. Gething, M.J. and J. Sambrook, *Protein folding in the cell.* Nature, 1992. **355**(6355): p. 33-45.
17. Chiti, F. and C.M. Dobson, *Protein misfolding, functional amyloid, and human disease.* Annu Rev Biochem, 2006. **75**: p. 333-66.
18. Alberts, B., *Molecular biology of the cell*. 4th ed. 2002, New York: Garland Science. xxxiv, 1548 p.
19. Buxbaum, J.N., et al., *Amyloid nomenclature 2022: update, novel proteins, and recommendations by the International Society of Amyloidosis (ISA) Nomenclature Committee.* Amyloid, 2022. **29**(4): p. 213-219.
20. Sipe, J.D. and A.S. Cohen, *Review: history of the amyloid fibril.* J Struct Biol, 2000. **130**(2-3): p. 88-98.
21. Greenwald, J. and R. Riek, *Biology of amyloid: structure, function, and regulation.* Structure, 2010. **18**(10): p. 1244-60.
22. Nelson, R., et al., *Structure of the cross-beta spine of amyloid-like fibrils.* Nature, 2005. **435**(7043): p. 773-8.
23. Morris, K.L. and L.C. Serpell, *X-ray fibre diffraction studies of amyloid fibrils.* Methods Mol Biol, 2012. **849**: p. 121-35.
24. Eanes, E.D. and G.G. Glenner, *X-ray diffraction studies on amyloid filaments.* J Histochem Cytochem, 1968. **16**(11): p. 673-7.

25. Chiti, F. and C.M. Dobson, *Protein Misfolding, Amyloid Formation, and Human Disease: A Summary of Progress Over the Last Decade.* Annu Rev Biochem, 2017. **86**: p. 27-68.
26. Polykretis, P., et al., *Exploring the Abeta(1-42) fibrillogenesis timeline by atomic force microscopy and surface enhanced Raman spectroscopy.* Front Mol Biosci, 2024. **11**: p. 1376411.
27. Fandrich, M., et al., *Amyloid fibril polymorphism: a challenge for molecular imaging and therapy.* J Intern Med, 2018. **283**(3): p. 218-237.
28. Gremer, L., et al., *Fibril structure of amyloid-beta(1-42) by cryo-electron microscopy.* Science, 2017. **358**(6359): p. 116-119.
29. Kollmer, M., et al., *Cryo-EM structure and polymorphism of Abeta amyloid fibrils purified from Alzheimer's brain tissue.* Nat Commun, 2019. **10**(1): p. 4760.
30. Yang, Y., et al., *Cryo-EM structures of amyloid-beta filaments with the Arctic mutation (E22G) from human and mouse brains.* Acta Neuropathol, 2023. **145**(3): p. 325-333.
31. Murphy, M.P. and H. LeVine, 3rd, *Alzheimer's disease and the amyloid-beta peptide.* J Alzheimers Dis, 2010. **19**(1): p. 311-23.
32. Yang, Y., et al., *Cryo-EM structures of amyloid-beta 42 filaments from human brains.* Science, 2022. **375**(6577): p. 167-172.
33. Dobson, C.M., *Protein folding and misfolding.* Nature, 2003. **426**(6968): p. 884-90.
34. Ruggeri, F.S., et al., *The Influence of Pathogenic Mutations in alpha-Synuclein on Biophysical and Structural Characteristics of Amyloid Fibrils.* ACS Nano, 2020. **14**(5): p. 5213-5222.
35. Chakraborty, P., et al., *GSK3beta phosphorylation catalyzes the aggregation of tau into Alzheimer's disease-like filaments.* Proc Natl Acad Sci U S A, 2024. **121**(52): p. e2414176121.
36. Kusumoto, Y., et al., *Temperature dependence of amyloid beta-protein fibrillization.* Proc Natl Acad Sci U S A, 1998. **95**(21): p. 12277-82.
37. Meisl, G., et al., *Quantitative analysis of intrinsic and extrinsic factors in the aggregation mechanism of Alzheimer-associated Abeta-peptide.* Sci Rep, 2016. **6**: p. 18728.
38. Dou, T. and D. Kurouski, *Phosphatidylcholine and Phosphatidylserine Uniquely Modify the Secondary Structure of alpha-Synuclein Oligomers Formed in Their Presence at the Early Stages of Protein Aggregation.* ACS Chem Neurosci, 2022. **13**(16): p. 2380-2385.
39. Sasanian, N., et al., *Ganglioside GM1 slows down Abeta(1-42) aggregation by a primary nucleation inhibitory mechanism that is modulated by sphingomyelin and cholesterol.* Commun Chem, 2025.
40. Sanderson, J.M., *The association of lipids with amyloid fibrils.* J Biol Chem, 2022. **298**(8): p. 102108.
41. Sasanian, N., et al., *Redox-Dependent Copper Ion Modulation of Amyloid-beta (1-42) Aggregation In Vitro.* Biomolecules, 2020. **10**(6).
42. Tao, J., et al., *Hsp70 chaperone blocks alpha-synuclein oligomer formation via a novel engagement mechanism.* J Biol Chem, 2021. **296**: p. 100613.
43. Halipi, V., et al., *Extracellular Vesicles Slow Down Aβ(1-42) Aggregation by Interfering with the Amyloid Fibril Elongation Step.* Acs Chemical Neuroscience, 2024. **15**(5): p. 944-954.
44. Yang, L., et al., *Decoding adipose-brain crosstalk: Distinct lipid cargo in human adipose-derived extracellular vesicles modulates amyloid aggregation in Alzheimer's disease.* Alzheimers Dement, 2025. **21**(10): p. e70603.
45. Vekrellis, K., et al., *Proteolytic activities of extracellular vesicles attenuate A-synuclein aggregation.* NPJ Parkinsons Dis, 2025. **11**(1): p. 277.
46. Morris, A.M., M.A. Watzky, and R.G. Finke, *Protein aggregation kinetics, mechanism, and curve-fitting: a review of the literature.* Biochim Biophys Acta, 2009. **1794**(3): p. 375-97.
47. Arosio, P., T.P. Knowles, and S. Linse, *On the lag phase in amyloid fibril formation.* Phys Chem Chem Phys, 2015. **17**(12): p. 7606-18.
48. Bemporad, F. and F. Chiti, *Protein misfolded oligomers: experimental approaches, mechanism of formation, and structure-toxicity relationships.* Chem Biol, 2012. **19**(3): p. 315-27.
49. Linse, S., *Toward the equilibrium and kinetics of amyloid peptide self-assembly.* Curr Opin Struct Biol, 2021. **70**: p. 87-98.
50. Scheltens, P., et al., *Alzheimer's disease.* Lancet, 2016. **388**(10043): p. 505-17.

51. Andrade-Guerrero, J., et al., *Alzheimer's Disease: An Updated Overview of Its Genetics.* Int J Mol Sci, 2023. **24**(4).
52. *2024 Alzheimer's disease facts and figures.* Alzheimers Dement, 2024. **20**(5): p. 3708-3821.
53. Silva, M.V.F., et al., *Alzheimer's disease: risk factors and potentially protective measures.* J Biomed Sci, 2019. **26**(1): p. 33.
54. Sims, J.R., et al., *Donanemab in Early Symptomatic Alzheimer Disease: The TRAILBLAZER-ALZ 2 Randomized Clinical Trial.* JAMA, 2023. **330**(6): p. 512-527.
55. Braak, E., et al., *Neuropathology of Alzheimer's disease: what is new since A. Alzheimer?* Eur Arch Psychiatry Clin Neurosci, 1999. **249 Suppl 3**: p. 14-22.
56. Tiwari, S., et al., *Alzheimer's disease: pathogenesis, diagnostics, and therapeutics.* Int J Nanomedicine, 2019. **14**: p. 5541-5554.
57. Das, U., et al., *Activity-induced convergence of APP and BACE-1 in acidic microdomains via an endocytosis-dependent pathway.* Neuron, 2013. **79**(3): p. 447-60.
58. Zhang, S., et al., *BACE1 Cleavage Site Selection Critical for Amyloidogenesis and Alzheimer's Pathogenesis.* J Neurosci, 2017. **37**(29): p. 6915-6925.
59. De Strooper, B., *Aph-1, Pen-2, and Nicastrin with Presenilin generate an active gamma-Secretase complex.* Neuron, 2003. **38**(1): p. 9-12.
60. Cole, S.L. and R. Vassar, *The Alzheimer's disease beta-secretase enzyme, BACE1.* Mol Neurodegener, 2007. **2**: p. 22.
61. Abelein, A., et al., *Molecular Structure of Cu(II)-Bound Amyloid-beta Monomer Implicated in Inhibition of Peptide Self-Assembly in Alzheimer's Disease.* JACS Au, 2022. **2**(11): p. 2571-2584.
62. Mager, P.P., *Molecular simulation of the primary and secondary structures of the Abeta(1-42)-peptide of Alzheimer's disease.* Med Res Rev, 1998. **18**(6): p. 403-30.
63. Liu, R., et al., *Residues 17-20 and 30-35 of beta-amyloid play critical roles in aggregation.* J Neurosci Res, 2004. **75**(2): p. 162-171.
64. Rezaei-Ghaleh, N., et al., *Familial Alzheimer's Disease-Related Mutations Differentially Alter Stability of Amyloid-Beta Aggregates.* J Phys Chem Lett, 2023. **14**(6): p. 1427-1435.
65. Knowles, T.P., M. Vendruscolo, and C.M. Dobson, *The amyloid state and its association with protein misfolding diseases.* Nat Rev Mol Cell Biol, 2014. **15**(6): p. 384-96.
66. Zimmermann, M.R., et al., *Mechanism of Secondary Nucleation at the Single Fibril Level from Direct Observations of Abeta42 Aggregation.* J Am Chem Soc, 2021. **143**(40): p. 16621-16629.
67. Lindberg, D.J., et al., *Steady-state and time-resolved Thioflavin-T fluorescence can report on morphological differences in amyloid fibrils formed by Abeta(1-40) and Abeta(1-42).* Biochem Biophys Res Commun, 2015. **458**(2): p. 418-23.
68. Thacker, D., et al., *Direct observation of secondary nucleation along the fibril surface of the amyloid beta 42 peptide.* Proc Natl Acad Sci U S A, 2023. **120**(25): p. e2220664120.
69. Haass, C. and D.J. Selkoe, *Soluble protein oligomers in neurodegeneration: lessons from the Alzheimer's amyloid beta-peptide.* Nat Rev Mol Cell Biol, 2007. **8**(2): p. 101-12.
70. Munke, A., et al., *Phage display and kinetic selection of antibodies that specifically inhibit amyloid self-replication.* Proc Natl Acad Sci U S A, 2017. **114**(25): p. 6444-6449.
71. Chavez-Gutierrez, L., et al., *The mechanism of gamma-Secretase dysfunction in familial Alzheimer disease.* EMBO J, 2012. **31**(10): p. 2261-74.
72. Varshavskaya, K.B., et al., *Post-translational modifications of beta-amyloid alter its transport in the blood-brain barrier in vitro model.* Front Mol Neurosci, 2024. **17**: p. 1362581.
73. Kummer, M.P. and M.T. Heneka, *Truncated and modified amyloid-beta species.* Alzheimers Res Ther, 2014. **6**(3): p. 28.
74. Jamasbi, E., et al., *Phosphorylation of a full length amyloid-beta peptide modulates its amyloid aggregation, cell binding and neurotoxic properties.* Mol Biosyst, 2017. **13**(8): p. 1545-1551.
75. Kumar, R., et al., *Identification of potential aggregation hotspots on Abeta42 fibrils blocked by the anti-amyloid chaperone-like BRICHOS domain.* Nat Commun, 2024. **15**(1): p. 965.
76. Yagi-Utsumi, M., et al., *The Double-Layered Structure of Amyloid-beta Assemblage on GM1-Containing Membranes Catalytically Promotes Fibrillization.* ACS Chem Neurosci, 2023. **14**(15): p. 2648-2657.

77. Rudajev, V. and J. Novotny, *Cholesterol as a key player in amyloid beta-mediated toxicity in Alzheimer's disease.* Front Mol Neurosci, 2022. **15**: p. 937056.
78. Mirdha, L., *Aggregation Behavior of Amyloid Beta Peptide Depends Upon the Membrane Lipid Composition.* J Membr Biol, 2024. **257**(3-4): p. 151-164.
79. Ye, F., et al., *Co-Aggregation of Syndecan-3 with beta-Amyloid Aggravates Neuroinflammation and Cognitive Impairment in 5xFAD Mice.* Int J Mol Sci, 2025. **26**(12).
80. Hampel, H., et al., *The Amyloid-beta Pathway in Alzheimer's Disease.* Mol Psychiatry, 2021. **26**(10): p. 5481-5503.
81. Mroczko, B., et al., *Amyloid beta oligomers (AbetaOs) in Alzheimer's disease.* J Neural Transm (Vienna), 2018. **125**(2): p. 177-191.
82. Braak, H. and E. Braak, *Neuropathological stageing of Alzheimer-related changes.* Acta Neuropathol, 1991. **82**(4): p. 239-59.
83. Zhang, H., et al., *Role of Abeta in Alzheimer's-related synaptic dysfunction.* Front Cell Dev Biol, 2022. **10**: p. 964075.
84. Ripoli, C., et al., *Intracellular accumulation of amyloid-beta (Abeta) protein plays a major role in Abeta-induced alterations of glutamatergic synaptic transmission and plasticity.* J Neurosci, 2014. **34**(38): p. 12893-903.
85. Lee, A., et al., *Abeta42 oligomers trigger synaptic loss through CAMKK2-AMPK-dependent effectors coordinating mitochondrial fission and mitophagy.* Nat Commun, 2022. **13**(1): p. 4444.
86. Meng, X., et al., *Neurotoxic beta-amyloid oligomers cause mitochondrial dysfunction-the trigger for PANoptosis in neurons.* Front Aging Neurosci, 2024. **16**: p. 1400544.
87. Merighi, S., et al., *Microglia and Alzheimer's Disease.* Int J Mol Sci, 2022. **23**(21).
88. Foret, M.K., et al., *Early oxidative stress and DNA damage in Abeta-burdened hippocampal neurons in an Alzheimer's-like transgenic rat model.* Commun Biol, 2024. **7**(1): p. 861.
89. Bai, R., et al., *Oxidative stress: The core pathogenesis and mechanism of Alzheimer's disease.* Ageing Res Rev, 2022. **77**: p. 101619.
90. Small, S.A., et al., *Endosomal Traffic Jams Represent a Pathogenic Hub and Therapeutic Target in Alzheimer's Disease.* Trends Neurosci, 2017. **40**(10): p. 592-602.
91. Wesen, E., et al., *Endocytic uptake of monomeric amyloid-beta peptides is clathrin- and dynamin-independent and results in selective accumulation of Abeta(1-42) compared to Abeta(1-40).* Sci Rep, 2017. **7**(1): p. 2021.
92. Cataldo, A.M., et al., *Endocytic pathway abnormalities precede amyloid beta deposition in sporadic Alzheimer's disease and Down syndrome: differential effects of APOE genotype and presenilin mutations.* Am J Pathol, 2000. **157**(1): p. 277-86.
93. Rajendran, L., et al., *Alzheimer's disease beta-amyloid peptides are released in association with exosomes.* Proc Natl Acad Sci U S A, 2006. **103**(30): p. 11172-7.
94. Shelke, G.V., et al., *Inhibition of endolysosome fusion increases exosome secretion.* J Cell Biol, 2023. **222**(6).
95. Berumen Sanchez, G., et al., *Extracellular vesicles: mediators of intercellular communication in tissue injury and disease.* Cell Commun Signal, 2021. **19**(1): p. 104.
96. Buzas, E.I., *The roles of extracellular vesicles in the immune system.* Nat Rev Immunol, 2023. **23**(4): p. 236-250.
97. Couch, Y., et al., *A brief history of nearly EV-erything - The rise and rise of extracellular vesicles.* J Extracell Vesicles, 2021. **10**(14): p. e12144.
98. Raposo, G., et al., *B lymphocytes secrete antigen-presenting vesicles.* J Exp Med, 1996. **183**(3): p. 1161-72.
99. Bard, M.P., et al., *Proteomic analysis of exosomes isolated from human malignant pleural effusions.* Am J Respir Cell Mol Biol, 2004. **31**(1): p. 114-21.
100. Subra, C., et al., *Exosome lipidomics unravels lipid sorting at the level of multivesicular bodies.* Biochimie, 2007. **89**(2): p. 205-12.
101. Skokos, D., et al., *Mast cell-derived exosomes induce phenotypic and functional maturation of dendritic cells and elicit specific immune responses in vivo.* J Immunol, 2003. **170**(6): p. 3037-45.

102. Joshi, P., et al., *Microglia convert aggregated amyloid-beta into neurotoxic forms through the shedding of microvesicles.* Cell Death Differ, 2014. **21**(4): p. 582-93.
103. Kumar, M.A., et al., *Extracellular vesicles as tools and targets in therapy for diseases.* Signal Transduct Target Ther, 2024. **9**(1): p. 27.
104. Welsh, J.A., et al., *Minimal information for studies of extracellular vesicles (MISEV2023): From basic to advanced approaches.* J Extracell Vesicles, 2024. **13**(2): p. e12404.
105. Babst, M., *MVB vesicle formation: ESCRT-dependent, ESCRT-independent and everything in between.* Curr Opin Cell Biol, 2011. **23**(4): p. 452-7.
106. Zhang, Y., et al., *Exosomes: biogenesis, biologic function and clinical potential.* Cell Biosci, 2019. **9**: p. 19.
107. Klumperman, J. and G. Raposo, *The complex ultrastructure of the endolysosomal system.* Cold Spring Harb Perspect Biol, 2014. **6**(10): p. a016857.
108. Airola, M.V. and Y.A. Hannun, *Sphingolipid metabolism and neutral sphingomyelinases.* Handb Exp Pharmacol, 2013(215): p. 57-76.
109. Wang, J., et al., *Surface Components and Biological Interactions of Extracellular Vesicles.* ACS Nano, 2025. **19**(9): p. 8433-8461.
110. Liu, Y.J. and C. Wang, *A review of the regulatory mechanisms of extracellular vesicles-mediated intercellular communication.* Cell Commun Signal, 2023. **21**(1): p. 77.
111. Fan, Y., et al., *Differential proteomics argues against a general role for CD9, CD81 or CD63 in the sorting of proteins into extracellular vesicles.* J Extracell Vesicles, 2023. **12**(8): p. e12352.
112. Lin, B., et al., *Tracing Tumor-Derived Exosomal PD-L1 by Dual-Aptamer Activated Proximity-Induced Droplet Digital PCR.* Angew Chem Int Ed Engl, 2021. **60**(14): p. 7582-7586.
113. Kalluri, R. and K.M. McAndrews, *The role of extracellular vesicles in cancer.* Cell, 2023. **186**(8): p. 1610-1626.
114. Ramachandran, A., R. Dhar, and A. Devi, *Stem Cell-Derived Exosomes: An Advanced Horizon to Cancer Regenerative Medicine.* ACS Appl Bio Mater, 2024. **7**(4): p. 2128-2139.
115. Skotland, T., et al., *An emerging focus on lipids in extracellular vesicles.* Adv Drug Deliv Rev, 2020. **159**: p. 308-321.
116. Ghadami, S. and K. Dellinger, *The lipid composition of extracellular vesicles: applications in diagnostics and therapeutic delivery.* Front Mol Biosci, 2023. **10**: p. 1198044.
117. Pfrieger, F.W. and N. Vitale, *Cholesterol and the journey of extracellular vesicles.* J Lipid Res, 2018. **59**(12): p. 2255-2261.
118. Sapon, K., et al., *The role of lipid rafts in vesicle formation.* J Cell Sci, 2023. **136**(9).
119. Hallal, S., et al., *Understanding the extracellular vesicle surface for clinical molecular biology.* J Extracell Vesicles, 2022. **11**(10): p. e12260.
120. Krokidis, M.G., et al., *Lipidomic Analysis of Plasma Extracellular Vesicles Derived from Alzheimer's Disease Patients.* Cells, 2024. **13**(8).
121. Cerezo-Magana, M., A. Bang-Rudenstam, and M. Belting, *The pleiotropic role of proteoglycans in extracellular vesicle mediated communication in the tumor microenvironment.* Semin Cancer Biol, 2020. **62**: p. 99-107.
122. Jia, L., et al., *Blood neuro-exosomal synaptic proteins predict Alzheimer's disease at the asymptomatic stage.* Alzheimers Dement, 2021. **17**(1): p. 49-60.
123. Wood, M.J., A.J. O'Loughlin, and L. Samira, *Exosomes and the blood-brain barrier: implications for neurological diseases.* Ther Deliv, 2011. **2**(9): p. 1095-9.
124. Sariano, P.A., et al., *Convection and extracellular matrix binding control interstitial transport of extracellular vesicles.* J Extracell Vesicles, 2023. **12**(4): p. e12323.
125. Schmidt, E.N., et al., *Siglec-6 mediates the uptake of extracellular vesicles through a noncanonical glycolipid binding pocket.* Nat Commun, 2023. **14**(1): p. 2327.
126. Elsharkasy, O.M., et al., *Integrin beta 1 and fibronectin mediate extracellular vesicle uptake and functional RNA delivery.* J Biol Chem, 2025. **301**(3): p. 108305.
127. Gonda, A., et al., *Internalization of Exosomes through Receptor-Mediated Endocytosis.* Mol Cancer Res, 2019. **17**(2): p. 337-347.
128. Christianson, H.C., et al., *Cancer cell exosomes depend on cell-surface heparan sulfate proteoglycans for their internalization and functional activity.* Proc Natl Acad Sci U S A, 2013. **110**(43): p. 17380-5.

129. Fitzner, D., et al., *Selective transfer of exosomes from oligodendrocytes to microglia by macropinocytosis.* J Cell Sci, 2011. **124**(Pt 3): p. 447-58.
130. Yanez-Mo, M., et al., *Biological properties of extracellular vesicles and their physiological functions.* J Extracell Vesicles, 2015. **4**: p. 27066.
131. Morelli, A.E., et al., *Endocytosis, intracellular sorting, and processing of exosomes by dendritic cells.* Blood, 2004. **104**(10): p. 3257-66.
132. O'Brien, K., et al., *Uptake, functionality, and re-release of extracellular vesicle-encapsulated cargo.* Cell Rep, 2022. **39**(2): p. 110651.
133. Joshi, B.S., et al., *Endocytosis of Extracellular Vesicles and Release of Their Cargo from Endosomes.* ACS Nano, 2020. **14**(4): p. 4444-4455.
134. Sardar Sinha, M., et al., *Alzheimer's disease pathology propagation by exosomes containing toxic amyloid-beta oligomers.* Acta Neuropathol, 2018. **136**(1): p. 41-56.
135. Wang, X. and G. Yang, *Bone marrow mesenchymal stem cells-derived exosomes reduce Abeta deposition and improve cognitive function recovery in mice with Alzheimer's disease by activating sphingosine kinase/sphingosine-1-phosphate signaling pathway.* Cell Biol Int, 2021. **45**(4): p. 775-784.
136. Hill, A.F., *Extracellular Vesicles and Neurodegenerative Diseases.* J Neurosci, 2019. **39**(47): p. 9269-9273.
137. Phelps, J., et al., *Extracellular Vesicles for the Treatment of Alzheimer's Disease: A Systematic Review.* J Extracell Biol, 2025. **4**(8): p. e70077.
138. Zhou, W., et al., *Stem cell-derived extracellular vesicles in the therapeutic intervention of Alzheimer's Disease, Parkinson's Disease, and stroke.* Theranostics, 2024. **14**(8): p. 3358-3384.
139. Cone, A.S., et al., *Mesenchymal stem cell-derived extracellular vesicles ameliorate Alzheimer's disease-like phenotypes in a preclinical mouse model.* Theranostics, 2021. **11**(17): p. 8129-8142.
140. Cui, G.H., et al., *RVG-modified exosomes derived from mesenchymal stem cells rescue memory deficits by regulating inflammatory responses in a mouse model of Alzheimer's disease.* Immun Ageing, 2019. **16**: p. 10.
141. Elia, C.A., et al., *Intracerebral Injection of Extracellular Vesicles from Mesenchymal Stem Cells Exerts Reduced Abeta Plaque Burden in Early Stages of a Preclinical Model of Alzheimer's Disease.* Cells, 2019. **8**(9).
142. Deng, H., et al., *Therapeutic Efficacy of Extracellular Vesicles Derived from Stem Cell for Alzheimer's Disease: A Meta-Analysis Study.* Front Biosci (Landmark Ed), 2024. **29**(9): p. 340.
143. Perez-Gonzalez, R., et al., *The exosome secretory pathway transports amyloid precursor protein carboxyl-terminal fragments from the cell into the brain extracellular space.* J Biol Chem, 2012. **287**(51): p. 43108-15.
144. Sharples, R.A., et al., *Inhibition of gamma-secretase causes increased secretion of amyloid precursor protein C-terminal fragments in association with exosomes.* FASEB J, 2008. **22**(5): p. 1469-78.
145. Wolfe, D.M., et al., *Autophagy failure in Alzheimer's disease and the role of defective lysosomal acidification.* Eur J Neurosci, 2013. **37**(12): p. 1949-61.
146. Lee, J.H., et al., *Presenilin 1 Maintains Lysosomal Ca(2+) Homeostasis via TRPML1 by Regulating vATPase-Mediated Lysosome Acidification.* Cell Rep, 2015. **12**(9): p. 1430-44.
147. Willen, K., et al., *Abeta accumulation causes MVB enlargement and is modelled by dominant negative VPS4A.* Mol Neurodegener, 2017. **12**(1): p. 61.
148. Eitan, E., et al., *Extracellular Vesicle-Associated Abeta Mediates Trans-Neuronal Bioenergetic and Ca(2+)-Handling Deficits in Alzheimer's Disease Models.* NPJ Aging Mech Dis, 2016. **2**: p. 16019-.
149. Yuyama, K., et al., *Sphingolipid-modulated exosome secretion promotes clearance of amyloid-beta by microglia.* J Biol Chem, 2012. **287**(14): p. 10977-89.
150. Coughlan, C., et al., *Specific Binding of Alzheimer's Abeta Peptides to Extracellular Vesicles.* Int J Mol Sci, 2024. **25**(7).
151. Dinkins, M.B., et al., *Exosome reduction in vivo is associated with lower amyloid plaque load in the 5XFAD mouse model of Alzheimer's disease.* Neurobiol Aging, 2014. **35**(8): p. 1792-800.

152. Yin, F., *Lipid metabolism and Alzheimer's disease: clinical evidence, mechanistic link and therapeutic promise.* FEBS J, 2023. **290**(6): p. 1420-1453.
153. Reddy, P.H., et al., *Differential loss of synaptic proteins in Alzheimer's disease: implications for synaptic dysfunction.* J Alzheimers Dis, 2005. **7**(2): p. 103-17; discussion 173-80.
154. Manczak, M., et al., *Mitochondria are a direct site of A beta accumulation in Alzheimer's disease neurons: implications for free radical generation and oxidative damage in disease progression.* Hum Mol Genet, 2006. **15**(9): p. 1437-49.
155. Ehehalt, R., et al., *Amyloidogenic processing of the Alzheimer beta-amyloid precursor protein depends on lipid rafts.* J Cell Biol, 2003. **160**(1): p. 113-23.
156. Krawczuk, D., A. Kulczynska-Przybik, and B. Mroczko, *The Potential Regulators of Amyloidogenic Pathway of APP Processing in Alzheimer's Disease.* Biomedicines, 2025. **13**(7).
157. Sawamura, N., et al., *Modulation of amyloid precursor protein cleavage by cellular sphingolipids.* J Biol Chem, 2004. **279**(12): p. 11984-91.
158. Kakio, A., et al., *Interactions of amyloid beta-protein with various gangliosides in raft-like membranes: importance of GM1 ganglioside-bound form as an endogenous seed for Alzheimer amyloid.* Biochemistry, 2002. **41**(23): p. 7385-90.
159. Hu, J., S. Linse, and E. Sparr, *Ganglioside Micelles Affect Amyloid beta Aggregation by Coassembly.* ACS Chem Neurosci, 2023. **14**(24): p. 4335-4343.
160. Yanagisawa, K., et al., *GM1 ganglioside-bound amyloid beta-protein (A beta): a possible form of preamyloid in Alzheimer's disease.* Nat Med, 1995. **1**(10): p. 1062-6.
161. Yuyama, K., et al., *Decreased amyloid-beta pathologies by intracerebral loading of glycosphingolipid-enriched exosomes in Alzheimer model mice.* J Biol Chem, 2014. **289**(35): p. 24488-98.
162. Su, H., et al., *Characterization of brain-derived extracellular vesicle lipids in Alzheimer's disease.* J Extracell Vesicles, 2021. **10**(7): p. e12089.
163. Su, H., et al., *Exploring the significance of lipids in Alzheimer's disease and the potential of extracellular vesicles.* Proteomics, 2024. **24**(11): p. e2300063.
164. Cohn, W., et al., *Multi-Omics Analysis of Microglial Extracellular Vesicles From Human Alzheimer's Disease Brain Tissue Reveals Disease-Associated Signatures.* Front Pharmacol, 2021. **12**: p. 766082.
165. Hellstrand, E., et al., *Amyloid beta-protein aggregation produces highly reproducible kinetic data and occurs by a two-phase process.* ACS Chem Neurosci, 2010. **1**(1): p. 13-8.
166. Abelein, A., et al., *High-yield Production of Amyloid-beta Peptide Enabled by a Customized Spider Silk Domain.* Sci Rep, 2020. **10**(1): p. 235.
167. LeVine, H., 3rd, *Thioflavine T interaction with synthetic Alzheimer's disease beta-amyloid peptides: detection of amyloid aggregation in solution.* Protein Sci, 1993. **2**(3): p. 404-10.
168. Xue, C., et al., *Thioflavin T as an amyloid dye: fibril quantification, optimal concentration and effect on aggregation.* R Soc Open Sci, 2017. **4**(1): p. 160696.
169. Lendel, C., et al., *Detergent-like interaction of Congo red with the amyloid beta peptide.* Biochemistry, 2010. **49**(7): p. 1358-60.
170. Hurtle, B., et al., *Live-cell visualization of tau aggregation in human neurons.* Commun Biol, 2024. **7**(1): p. 1143.
171. Kreutzer, A.G., et al., *Antibodies Raised Against an Abeta Oligomer Mimic Recognize Pathological Features in Alzheimer's Disease and Associated Amyloid-Disease Brain Tissue.* ACS Cent Sci, 2024. **10**(1): p. 104-121.
172. Meisl, G., et al., *Differences in nucleation behavior underlie the contrasting aggregation kinetics of the Abeta40 and Abeta42 peptides.* Proc Natl Acad Sci U S A, 2014. **111**(26): p. 9384-9.
173. Arosio, P., et al., *Quantification of the concentration of Abeta42 propagons during the lag phase by an amyloid chain reaction assay.* J Am Chem Soc, 2014. **136**(1): p. 219-25.
174. Lehrich, B.M., Y. Liang, and M.S. Fiandaca, *Foetal bovine serum influence on in vitro extracellular vesicle analyses.* J Extracell Vesicles, 2021. **10**(3): p. e12061.
175. Gross, J., et al., *Nanoparticle tracking analysis of particle size and concentration detection in suspensions of polymer and protein samples: Influence of experimental and data evaluation parameters.* Eur J Pharm Biopharm, 2016. **104**: p. 30-41.

176. Thakur, A., et al., *The mini player with diverse functions: extracellular vesicles in cell biology, disease, and therapeutics.* Protein Cell, 2022. **13**(9): p. 631-654.
177. Zhang, X., et al., *Correlation between Cellular Uptake and Cytotoxicity of Fragmented alpha-Synuclein Amyloid Fibrils Suggests Intracellular Basis for Toxicity.* ACS Chem Neurosci, 2020. **11**(3): p. 233-241.
178. Xue, W.F., et al., *Fibril fragmentation enhances amyloid cytotoxicity.* J Biol Chem, 2009. **284**(49): p. 34272-82.
179. Smith, R.A., et al., *Analysis of Toxic Amyloid Fibril Interactions at Natively Derived Membranes by Ellipsometry.* PLoS One, 2015. **10**(7): p. e0132309.
180. Toth, E.A., et al., *Formation of a protein corona on the surface of extracellular vesicles in blood plasma.* J Extracell Vesicles, 2021. **10**(11): p. e12140.
181. Dietz, L., et al., *Uptake of extracellular vesicles into immune cells is enhanced by the protein corona.* J Extracell Vesicles, 2023. **12**(12): p. e12399.
182. Wolf, M., et al., *A functional corona around extracellular vesicles enhances angiogenesis, skin regeneration and immunomodulation.* J Extracell Vesicles, 2022. **11**(4): p. e12207.
183. Choi, D., et al., *Quantitative proteomic analysis of trypsin-treated extracellular vesicles to identify the real-vesicular proteins.* J Extracell Vesicles, 2020. **9**(1): p. 1757209.
184. Liu, X., et al., *Intraluminal proteome and peptidome of human urinary extracellular vesicles.* Proteomics Clin Appl, 2015. **9**(5-6): p. 568-73.
185. Lakowicz, J.R., *Principles of fluorescence spectroscopy*. 3rd ed. 2006, New York: Springer. xxvi, 954 p.
186. Snow, A.D., et al., *Heparan sulfate proteoglycan in diffuse plaques of hippocampus but not of cerebellum in Alzheimer's disease brain.* Am J Pathol, 1994. **144**(2): p. 337-47.
187. Wesen, E., et al., *Cell surface proteoglycan-mediated uptake and accumulation of the Alzheimer's disease peptide Abeta(1-42).* Biochim Biophys Acta Biomembr, 2018. **1860**(11): p. 2204-2214.
188. Sandwall, E., et al., *Heparan sulfate mediates amyloid-beta internalization and cytotoxicity.* Glycobiology, 2010. **20**(5): p. 533-41.
189. Snow, A.D., et al., *Early accumulation of heparan sulfate in neurons and in the beta-amyloid protein-containing lesions of Alzheimer's disease and Down's syndrome.* Am J Pathol, 1990. **137**(5): p. 1253-70.
190. Esko, J.D., T.E. Stewart, and W.H. Taylor, *Animal cell mutants defective in glycosaminoglycan biosynthesis.* Proc Natl Acad Sci U S A, 1985. **82**(10): p. 3197-201.
191. Kaya, I., et al., *Delineating Amyloid Plaque Associated Neuronal Sphingolipids in Transgenic Alzheimer's Disease Mice (tgArcSwe) Using MALDI Imaging Mass Spectrometry.* ACS Chem Neurosci, 2017. **8**(2): p. 347-355.
192. Di Paolo, G. and T.W. Kim, *Linking lipids to Alzheimer's disease: cholesterol and beyond.* Nat Rev Neurosci, 2011. **12**(5): p. 284-96.
193. Lingwood, D. and K. Simons, *Lipid rafts as a membrane-organizing principle.* Science, 2010. **327**(5961): p. 46-50.
194. Skotland, T., K. Sandvig, and A. Llorente, *Lipids in exosomes: Current knowledge and the way forward.* Prog Lipid Res, 2017. **66**: p. 30-41.
195. Gurung, S., et al., *The exosome journey: from biogenesis to uptake and intracellular signalling.* Cell Commun Signal, 2021. **19**(1): p. 47.
196. Habchi, J., et al., *Cholesterol catalyses Abeta42 aggregation through a heterogeneous nucleation pathway in the presence of lipid membranes.* Nat Chem, 2018. **10**(6): p. 673-683.
197. Longo, A., et al., *Extracellular Vesicles in the Crosstalk of Autophagy and Apoptosis: A Role for Lipid Rafts.* Cells, 2025. **14**(10).
198. Pait, M.C., et al., *Novel method for collecting hippocampal interstitial fluid extracellular vesicles (EV(ISF)) reveals sex-dependent changes in microglial EV proteome in response to Abeta pathology.* J Extracell Vesicles, 2024. **13**(1): p. e12398.
199. Lim, C.Z.J., et al., *Subtyping of circulating exosome-bound amyloid beta reflects brain plaque deposition.* Nat Commun, 2019. **10**(1): p. 1144.
200. Ngolab, J., et al., *Brain-derived exosomes from dementia with Lewy bodies propagate alpha-synuclein pathology.* Acta Neuropathol Commun, 2017. **5**(1): p. 46.

201. Liu, L., et al., *Discovery of lipid profiles in plasma-derived extracellular vesicles as biomarkers for breast cancer diagnosis.* Cancer Sci, 2023. **114**(10): p. 4020-4031.
202. Manganelli, V., et al., *Autophagy Promotes Enrichment of Raft Components within Extracellular Vesicles Secreted by Human 2FTGH Cells.* Int J Mol Sci, 2024. **25**(11).
203. Hosseinkhani, B., et al., *(Sub)populations of extracellular vesicles released by TNF-alpha - triggered human endothelial cells promote vascular inflammation and monocyte migration.* J Extracell Vesicles, 2020. **9**(1): p. 1801153.
204. Harold, D., et al., *Genome-wide association study identifies variants at CLU and PICALM associated with Alzheimer's disease.* Nat Genet, 2009. **41**(10): p. 1088-93.
205. Lambert, J.C., et al., *Meta-analysis of 74,046 individuals identifies 11 new susceptibility loci for Alzheimer's disease.* Nat Genet, 2013. **45**(12): p. 1452-8.
206. Rai, A., et al., *Proteomic dissection of large extracellular vesicle surfaceome unravels interactive surface platform.* J Extracell Vesicles, 2021. **10**(13): p. e12164.
207. Iha, K., et al., *Gastric Cancer Cell-Derived Exosomal GRP78 Enhances Angiogenesis upon Stimulation of Vascular Endothelial Cells.* Curr Issues Mol Biol, 2022. **44**(12): p. 6145-6157.
208. Lu, R.C., et al., *Heat shock protein 70 in Alzheimer's disease.* Biomed Res Int, 2014. **2014**: p. 435203.
209. Yoo, Y., et al., *Amyloid-beta-activated human microglial cells through ER-resident proteins.* J Proteome Res, 2015. **14**(1): p. 214-23.
210. Beloribi, S., et al., *Exosomal lipids impact notch signaling and induce death of human pancreatic tumoral SOJ-6 cells.* PLoS One, 2012. **7**(10): p. e47480.
211. Ahlberg, E., et al., *Proteome characterization of extracellular vesicles from human milk: Uncovering the surfaceome by a lipid-based protein immobilization technology.* J Extracell Biol, 2024. **3**(11): p. e70020.
212. Trajkovic, K., et al., *Ceramide triggers budding of exosome vesicles into multivesicular endosomes.* Science, 2008. **319**(5867): p. 1244-7.
213. Muraoka, S., et al., *Proteomic and biological profiling of extracellular vesicles from Alzheimer's disease human brain tissues.* Alzheimers Dement, 2020. **16**(6): p. 896-907.
214. Bodart-Santos, V., et al., *Alzheimer's disease brain-derived extracellular vesicles reveal altered synapse-related proteome and induce cognitive impairment in mice.* Alzheimers Dement, 2023. **19**(12): p. 5418-5436.